A Geomechanically-Constrained Dynamic Fractal Wormhole Growth Model for Simulating Cold Heavy Oil Production with Sand (CHOPS)

by

Haisheng Yu

A thesis submitted in partial fulfillment of the requirements for the degree of

Master of Science

in

Petroleum Engineering

Department of Civil and Environmental Engineering
University of Alberta

Abstract

Cold heavy oil production with sand (CHOPS) is a non-thermal primary process that is widely adopted in many weakly consolidated heavy oil deposits around the world. However, only approximately 5 to 15% of the initial oil in place is typically recovered. Several solvent-assisted schemes are proposed as follow-up strategies to increase the recovery factor in post-CHOPS operations. The development of complex, heterogeneous, high-permeability channels or wormholes during CHOPS renders the analysis and scalability of these processes challenging. One of the key issues is how to properly estimate the dynamic growth of wormholes during CHOPS. Existing growth models generally offer a simplified representation of the wormhole network, which, in many cases, is denoted as an extended wellbore. Despite it is commonly acknowledged that wormhole growth due to sand failure is likely to follow fractal statistics, there are no established workflows to incorporate geo-mechanical constraints into the construction of these fractal wormhole patterns.

A novel dynamic wormhole growth model is developed to generate a set of realistic fractal wormhole networks during the CHOPS operations. It offers an improvement to the commonly-adopted Diffusion Limited Aggregation (DLA) algorithm with a sand-arch-stability criterion. The outcome is a fractal pattern that mimics a realistic wormhole growth path, with sand failure and fluidization being controlled by geo-mechanical constraints. The fractal pattern is updated dynamically by coupling compositional flow simulation on a locally-refined grid and a stability criterion for the sand arch: the wormhole would continue expanding following the fractal pattern, provided that the pressure gradient at the tip exceeds the limit corresponding to a sand-arch-

stability criterion. Important transport mechanisms including foamy oil (non-equilibrium dissolution of gas) and sand failure are integrated.

Public field data for several CHOPS fields in Canada is used to examine the results of the dynamic wormhole growth model and flow simulations. For example, sand production history is used to estimate a practical range for the critical pressure gradient that represents the sand-arch-stability criterion. The oil and sand production histories show good agreement with the modeling results.

In many CHOPS or post-CHOPS modeling studies, constant wormhole intensity is commonly assigned uniformly throughout the entire domain; as a result, the ensuing models are unlikely to capture the complex heterogeneous distribution of wormholes encountered in realistic reservoir settings. This work, however, proposes a novel model to integrate a set of statistical fractal patterns with realistic geo-mechanical constraints. The entire workflow can be readily integrated with commercial reservoir simulators, enabling it to be incorporated in practical field-scale operations design.

Dedication

To my ever loving and devoting parents, Jiasheng Yu and Heqin Bai

Acknowledgements

I would like to express my sincere gratitude to my supervisor, Dr. Juliana Y. Leung. I feel extremely fortunate to have the opportunity to study with her. Without her patient instruction and guidance, the present research work would not possible to be accomplished. I thank her for the constant encouragement, guidance and always providing fascinating research ideas throughout my project with her patience. I learnt from her to see what research is, and how to be a stellar researcher. No matter when I encountered difficulties or lots, she always helps me with useful suggestions and patience. I know I must have given her lots of troubles over two years, but she always guided me to the right track. I really feel honored to have this opportunity to work with her.

I would also to express my special gratitude to Dr. Zhehui (Charlie) Jin, Dr. Nobuo Maeda and Dr. Wei (Victor) Liu for being part of my examination committee. Their constructive suggestions are always appreciated.

I am thankful for the friendship and technical support from my colleagues in the research group. Thanks for their suggestions, ideas, and encouragement.

Last but not the least, my special thank goes to my family, for their unwavering support throughout my life. To my wife, Lu, for her love, support, help, and sacrifice. She always encourages me in times of difficulties. To my sister, thank you for your love, friendship, and support. To my parents, whom I owe everything in life, for their unconditional love, continuous encouragement, and endless support.

Table of Contents

List of Tables

List of Figures

Nomenclature

Symbols

Cu	=	unconfined compressive strength (kPa)
Rc	=	average radius of curvature (m)
z_{max}	=	major axis of the ellipsoid
x_{max}	=	minor axis of the ellipsoid
r_d^1, r_d^2	=	transfer rate of solution gas into dispersed gas bubbles
N_1, N_2	=	mass Transfer rates for the kinetic reactions
G_1, G_2	=	transfer coefficients for the kinetic reactions
μ_o	=	oil phase viscosity
μ_{oi}	=	viscosity of component i in the liquid phase
f_{oi}	=	weighting factor corresponding to component i
P	=	reservoir pressure (kPa)
T	=	reservoir temperature (℃)
V_{crit}	=	critical oil phase velocity (m/day)
V	=	oil phase velocity (m/day)

V_{ref}	=	reference velocity for reaction rate (m/day)
Φ	=	scalar field
ϕ	=	reservoir porosity (fraction)

Subscripts

o	=	oil phase
oi	=	component *i* in the liquid phase
g	=	gas phase
gd	=	dissolved gas
bd	=	dispersed gas bubble

Acronyms

CHOPS	=	Cold Heavy Oil Production with Sand
UCSS	=	Unconsolidated Sandstone
PCPS	=	Progressive Cavity Pumps
DLA	=	Diffusion-Limited Aggregation
EOR	=	Enhanced Oil Recovery

UCS	=	Unconfined Compressive Strength

Chapter 1. Introduction

1.1 Background and Motivation

With increasing world's energy demand, heavy oil production has become increasingly important in recent years and shared the increasing percentage of the total petroleum supply. Due to the lower mobility, recovery of heavy oil (which is defined herein to be oils with API gravity ≤ 20° API and viscosity ≥ 10,000 cP (NEB, 2000) typically requires the injection of steam and/or solvent in various thermal or non-thermal methods. One of the world's largest oil deposits are the heavy and extra heavy oil deposits of Canada. Although various thermal recovery methods can be implemented effectively with proper design, the exceptionally high operating cost is still a significant factor in the consideration of real-field applications (Han et al., 2007). In addition, many thin and unconsolidated sand reservoirs in the Canada's western provinces of Alberta and Saskatchewan are not suitable candidates for steam and/or solvent injection due to excessive heat loss to the over/underburden; on the other hand, CHOPS have been applied successfully in such areas, which is the focus of this thesis.

Cold heavy oil production with sand (CHOPS) is a non-thermal primary process that is widely implemented in many weakly consolidated heavy oil deposits around the world. CHOPS technology was first introduced in the late 1980's in Canada and has developed and matured in the late 1990's. The development and adoption of progressively cavity pumps (PCPs) are important for handling a large amount of produced sand. In Canada, the cold production fields, which are mainly located along the Alberta and Saskatchewan heavy oil belt would account for

approximately 22% of the country's total petroleum production (~ 460,000 bbl/day) (DOE, 2002). In the past, excessive sand production was perceived to be detrimental and was deliberately avoided using sand exclusion devices (Geilikman et al., 1994). However, various operators were surprised by the surge in oil production (up to 10 times) after removing the sand exclusion devices in the Lloydminster area, Canada, in the late 1920s (Lougheand and Saltuklaroglu, 1992; Tremblay et al., 1999b). Field observations, tracer tests, and lab experiments seemed to reveal a direct correlation between oil and sand production rates; in fact, the enhancement in oil production is primarily attributed to the formation of a highly-conductive network of wormholes (Smith 1988; Yeung 1992; Metwally and Solanki, 1995). Sand production leads to the formation of many high-permeability channels (i.e., wormholes) around the wellbore. This network of highly-permeable channels could extend up to hundreds of meters away from the well. Another important physical mechanism in CHOPS production is foamy oil flow. As the reservoir pressure depletes below the bubble point during production, the dissolved gas will evolve from the heavy oil. However, due to the high molecular weight and viscosity of the liquid phase, formation of the continuous gas phase is delayed; the gas would be entrained as small bubbles in the oil (liquid) phase for a certain period of time. Therefore, foamy oil essentially describes the non-equilibrium phenomenon of the delay in gas dissolution. The presence of gas bubbles in an oil-continuous foam can lower the effective oil viscosity, hence enhancing the mobility of the oil phase.

Despite its low cost and practical heavy oil recovery technology, CHOPS becomes uneconomic after only 5 - 15% of the OOIP with the average recovery factor equal to 10% was recovered. That means a considerable amount of oil remains in the reservoir at the end of CHOPS operations. Also the CHOPS is a fully field driven technology which is not based on laboratory experiments, reservoir simulations or field plots done a priori from the production period.

Incorporating the growth of wormhole network in numerical simulation has been a subject of continual research. Existing growth models generally offer a simplified representation of the wormhole network. In many models, wormhole is represented as an extended wellbore (Istchenko and Gates, 2014) or as a region of enhanced permeability surrounding the wellbore (Rivero et al., 2010). Liu and Zhao (2005) proposed that the fractal wormhole model would be used to describe the characteristics of the wormhole structures. In this approach, the sand production data was used to determine the possible range of the wormhole network with the wormhole diameter determined by the Area Version of Gaussian Function. However, this fractal wormhole model can not capture the main mechanism with inability to demonstrate the preferential direction of wormhole growth. Despite it is commonly acknowledged that wormhole growth due to sand failure is likely to follow fractal statistics, there are no established models/workflows to incorporate both geo-mechanical constraints and fluid flows directly into the construction of wormhole patterns that are consistent with fractal statistics. Therefore, there is a need to formulate a new procedure for simulating fractal wormhole networks dynamically during the CHOPS operations.

1.2 Problem Statement

One of the key challenges pertinent to the numerical simulation of CHOPS is how to model the dynamic growth of wormholes by incorporating geomechanical constraints of sand failure, fractal patterns, and fluid flows. The distribution of wormhole networks has a significant effect on the in-situ stress distribution, liquefaction, and reservoir connectivity. The development of uncertain, complex, heterogeneous wormholes during CHOPS also renders the analysis and scalability of any post-CHOPS processes extremely difficult. In many CHOPS or post-CHOPS modeling studies,

constant wormhole intensity is commonly assigned uniformly throughout the entire domain; as a result, the ensuing models are unlikely to capture the complex heterogeneous distribution of wormholes encountered in realistic reservoir settings.

1.3 Research Objective

This thesis proposes a novel dynamic wormhole growth model by integrating a set of statistical fractal patterns with realistic geo-mechanical constraints and pressure depletion due to fluid flows.

Diffusion Limited Aggregation (DLA) algorithm is commonly adopted to generate a static fractal network; this work, however, would offer an improvement by controlling the fractal network generated using the DLA method with a sand-arch-stability criterion governed by geomechanics. The outcome is a fractal pattern that mimics a realistic wormhole growth path, with sand failure and fluidization being controlled by geo-mechanical constraints. As the simulation progresses, the fractal pattern is updated dynamically by coupling compositional flow simulation on a locally-refined grid and a stability criterion for the sand arch: the wormhole would continue expanding following the fractal pattern, provided that the pressure gradient at the tip exceeds the limit corresponding to a sand-arch-stability criterion. The corresponding oil and sand production at each time step will be computed. The specific objectives have been addressed below:

1) Propose a novel dynamic wormhole growth model for integrating a set of statistical fractal patterns with the realistic geomechanical constraints.
2) Integrate relevant transport mechanisms including foamy oil (non-equilibrium dissolution of gas).
3) Validate the proposed model by comparing with CHOPS field data in the literature.

4) Assess the performance of the proposed method (advantages and disadvantages) against several existing modeling strategies in the literature.
5) Perform sensitivity analysis with the validated model to examine the impacts of anisotropic stress distribution on the development of wormhole networks.

1.4 Thesis Outline

Chapter 1 presents the background and motivation related to this research, including the problem description and the specific research objectives that should be achieved.

Chapter 2 reviews the current literature for Cold Heavy Oil Production with Sand (CHOPS). This chapter starts with the comprehensive overview of CHOPS process, including the historical development of CHOPS technology and the typical production profiles. The chapter then summarizes the two of the main mechanisms in CHOPS reservoirs, and introduce different related approaches to modeling those mechanisms in models. Different approaches to modeling the CHOPS are summarized in the last section. A critical discussion of the strength and weakness of various existing CHOPS models have been listed in this chapter.

Chapter 3 presents the mythology that documented in this thesis in the development of our novel workflow to simulate the CHOPS process, including the approaches to model the foamy oil behavior, sand failure criterion, and sand production model. An entire workflow is introduced in details as well as the coupling strategy.

Chapter 4 summarizes the results of field production data and validation of the proposed CHOPS model by comparing with the CHOPS field history data. Assess the performance of our entire

workflow (advantages and disadvantages) against with other existing CHOPS models is also present. The proposed validated model is tested against with anisotropic stresses to examine the effect on the development of wormhole networks.

Chapter 5 finally presents the conclusion and recommendations for future work.

Chapter 2. Literature Review

2.1 Overview of Cold Heavy Oil Production with Sand (CHOPS)

Thermal recovery techniques, including steam-assisted gravity drainage (SAGD), cyclic steam stimulation, or steam flooding, are some of the most commonly adopted recovery methods for heavy oil reservoirs around the world. However, certain heavy oil deposits located in Western Canada and Venezuela, for example, are not suitable candidates for these aforementioned thermal methods for various reasons. These heavy oil deposits mainly consist of unconsolidated sandstones (UCSS, $\varphi \approx 30\%$) formations at shallow depths of 350-1000 m with oil viscosity ranging from 500 to 2,0000 cP at reservoir temperature. Sand production and excessive heat loss to overburden and underburden render these thermal technologies to be rather inefficient. As a result, many of these heavy oil reservoirs are not suitable candidates for exploitation with horizontal wells and typical thermal processes. The Luseland field in Saskatchewan is a case in point: it was produced in a conventional fashion with horizontal wells for 12 to 15 years before it was converted to CHOPS. The production histories from 1982 to 2000 are illustrated in **Figure 2-1**; the oil production has increased by almost four folds after the implementation of CHOPS with roughly the same number of the wells since 1984; it is obvious that the increment in the oil production was attributed to the CHOPS operations.

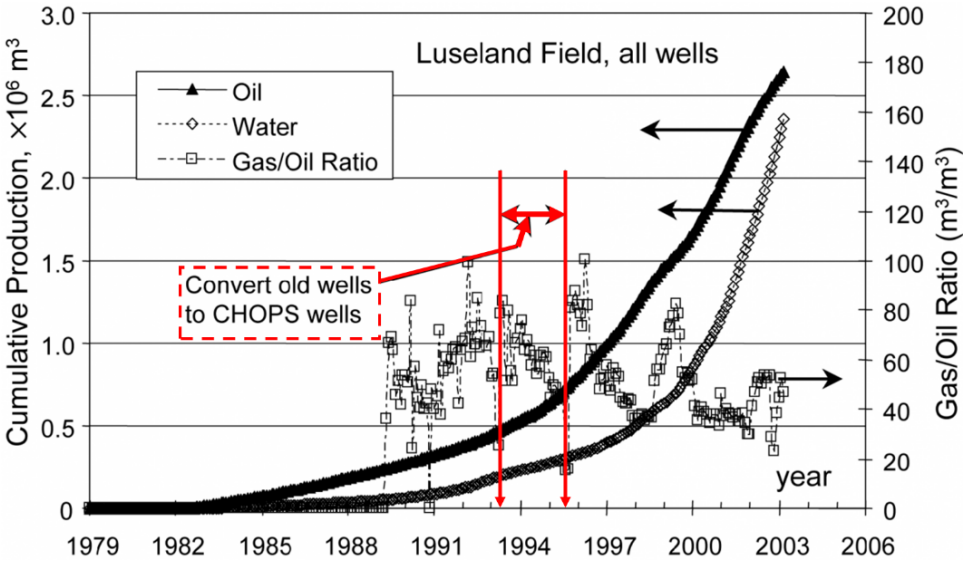

Figure 2-1: Luseland production history (Adapted from Glendasmith, 2012)

In Canada, these heavy oil deposits are located along the heavy oil belt in the Lloydminster area, Lindberg and Cold Lake areas, as shown in **Figure 2-2**. As opposed to the Athabasca bitumen, where in-situ oil viscosity exceeds 100,000 cP, the in-situ fluid viscosity in these reservoirs is approximately 10,000 cP at in-situ reservoir conditions. As a result, both oil and sand would flow towards the wellbore via primary (pressure) depletion. In the past, sand exclusion devices were installed to mitigate the adverse effects of sand production. However, operators subsequently observed that the oil production rate could be increased up to 10 times after the removal of such devices from numerous wellbores (Loughead and Saltuklaroglu, 1992). Several local operators confirmed that production in wells tended to surge upon removal of the sand exclusion devices (e.g., screens, liners, gravel packs). This observation suggested that sand production could potentially enhance the oil production. Since then, cold production with sand has become an important non-thermal recovery strategy in this area, and it is widely known as the Cold Heavy Oil Production with Sand (CHOPS).

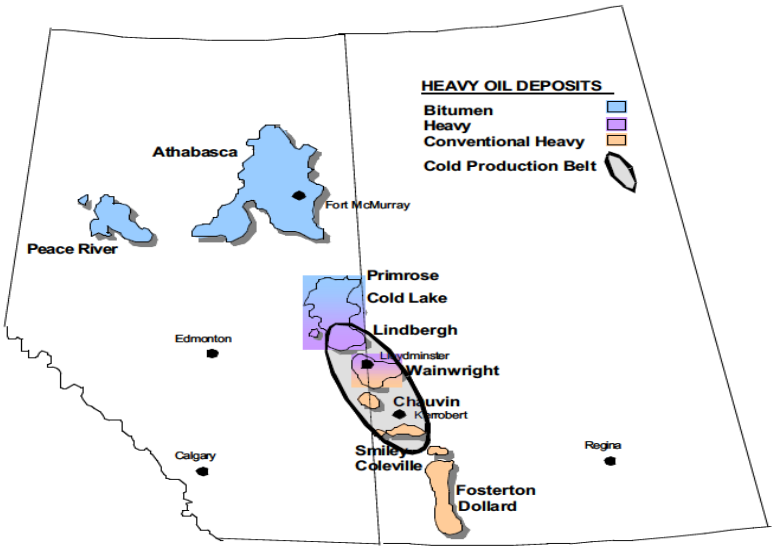

Figure 2-2: Heavy oil deposits in Western Canada with CHOPS assets shown (adapted from Sawatzky et al, 2002)

Well productivity was still limited by pump rate and upgrading capacity until the advent of progressive cavity pumps (PCPS) in the 1980's. With the development and adoption of PCP, operators could handle larger pressure drawdown and the associated sand volumes, while maximizing the oil production (Istchenko and Gates, 2014). As the operating cost continued to decline over the past three decades, this recovery technique has been incrementally implemented in other unconsolidated sandstone reservoirs elsewhere: for example, Venezuela (Orinoco belt), Russian and China (Liaohe Oilfield) (Huang et al., 1998; Tremblay et al., 1999).

A typical recovery factor for CHOPS is approximately 5-15% of the original oil in place. The reason for this relatively low recovery factor is that oil productivity is correlated to the sand production, which is a pressure-driven process; as the reservoir pressure is depleted, there is insufficient pressure gradient within the reservoir to induce further sand failure, and at that point, wormhole growth and sand production would cease. Follow-up or post-CHOPS strategies, which

often involve (co-) injection of steam and solvent, have been widely advocated to recover additional oil after the CHOPS stage.

An example of a typical CHOPS production profile is shown in **Figure 2-3**. A few salient features can be observed: (1) Sand rate is higher during the initial stage of production; the peak sand rate is approximately 15 to 40% of the volumetric oil rate; the sand rate gradually declines to a stabilized level (0.5-10%) over the course of several days to months. (2) Oil rate increases to a peak value in a fashion similar to that of the sand production rate, except for a slight delay; it also slowly declines as the reservoir depletes. This observation supports the notion that sand production is positively correlated with the oil production. The oil in the formation will continue to flow towards the wellbore through the established wormhole network, but there is insufficient pressure gradient to induce further sand failure and wormhole growth as pressure depletes. Optimal workover strategies could be implemented to promote more sand production, and multiple production cycles are often employed to boost the oil production **(Figure 2-4)**.

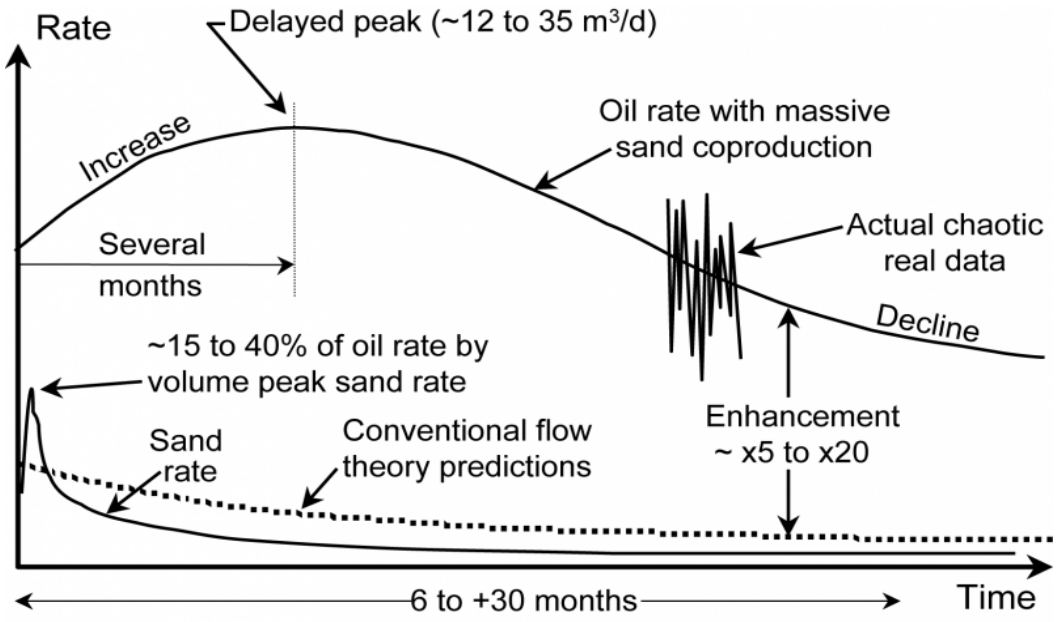

Figure 2-3: Typical CHOPS well production profile

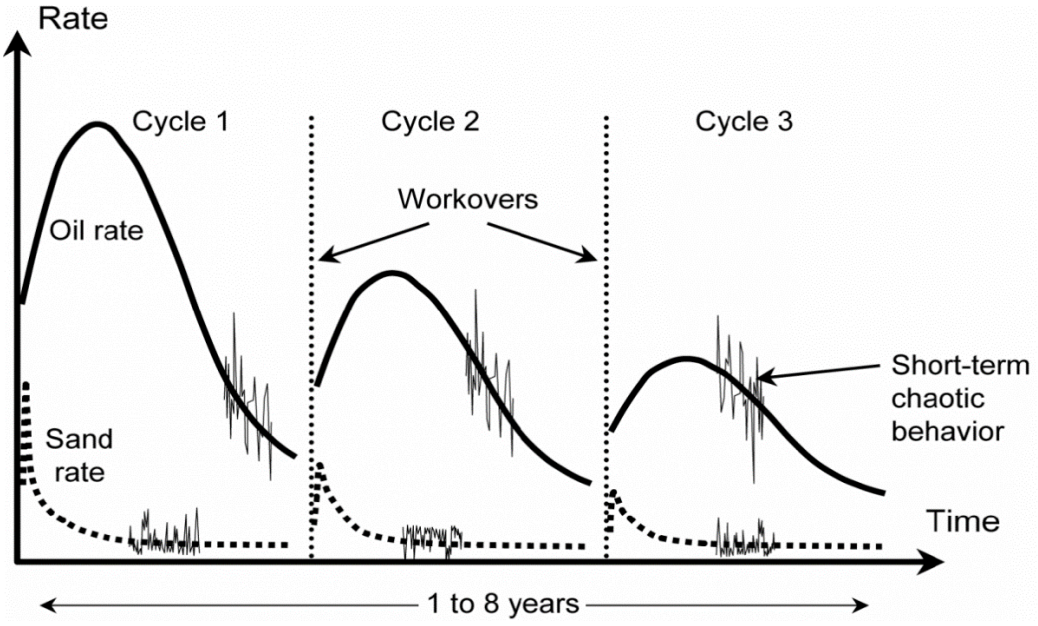

Figure 2-4: CHOPS well behavior over three production cycles

2.2 Enhanced Permeability Zone

In the CHOPS process, a set of driving forces is responsible for the continuous sand production that leads to the growth of a distributed zone of high porosity and permeability around the wellbore. The main mechanisms include the gravitational forces, natural fluid pressure gradients and foamy oil phenomena. In the porous medium, sand failure happens when the hydrodynamic drag force exceeds the sand bonding cohesion stress. In addition, natural fluid pressure gradients may cause the sand grains to disassociate from the unconsolidated sandstone and suspend in the flowing fluid. On the other hand, the foamy oil flow phenomenon, which contributes to reservoir pressure maintenance, would also liquefy and help keeping the sand particles in suspension.

They are a various field and laboratory studies which indicated the formation of the wormholes in CHOPS. Responses from field tracer injection tests in the Burnt Lake and Lloydminster reservoirs strongly supported the inferred presence of extensive wormholes around the wellbore (Squires, 1993 and Jensen, 1995). In the Burnt Lake field, some wells experienced damages in the shale cap rock, which were hypothesized as the result of sand production and subsequent changes in the in-situ stress conditions (Yeung, 1995). In the Clearwater reservoir near Elk Point Field, which was operated by Amoco Canada, the average cumulative sand production was 3.3% of the cumulative oil production, with produced sand volume exceeding 1,000m^3(Squires, 1993). Tracer injection tests were performed in an attempt to explain this high sand production. After 18 hours, the dye was observed at a distance of 2km away from the well locations (Squires, 1993 and Jensen, 1995). In addition, it was recorded that the dye was traveling at velocities that were up to 7m/min (Squires, 1993 and Jensen, 1995). In the end, the tracer dye was observed in 12 different wells, which was believed to be connected within a wormhole or channel system extending over 2km laterally (Squires, 1993). Results of subsequent pressure build-up tests, well logging and 4D seismic

surveys would all corroborate the existence of these high-conductivity channels around the wellbores (Loughead and Saltuklaroglu, 1992; Metwally and Solanki, 1995 and Yeung, 1992).

In addition to field observations, numerous laboratory experiments (Tremblay et al., 1996, 1997 and 1998) were conducted to demonstrate and study the growth of wormhole networks during primary depletion in CHOPS reservoirs. A sand pack with an orifice located at one end was used to simulate the oil and sand productions at constant flow rates. A high-permeability (wormhole) channel was observed in the sand pack based on computer tomography (CT). The role of gas dissolution in wormhole development was also examined (Tremblay et al., 1999). Their results demonstrated that the critical pressure gradient required for sand failure within a sandpack is significantly lower for the live oil sample (more dissolved gas) than for the dead oil (no dissolved gas) sample (Tremblay et al., 1999). Therefore, it was concluded that the release of the gas bubbles during depressurization is beneficial to the wormhole growth, as it helps to lower the apparent critical pressure gradient.

Details of the sand failure mechanism and wormhole growth in the CHOPS reservoirs will be presented in section 2.3.

2.3 Physical Mechanisms of CHOPS

In this section, two of the most significant recovery mechanisms in CHOPS reservoirs, including the development of high-permeability channels (wormholes) around the wellbore caused by foamy oil flow and sand production, will be discussed (Tremblay, 2005).

2.3.1 Foamy Oil Flow

In conventional oil reservoirs, as the pressure drops below the bubble point, gas will evolve as a separate phase in equilibrium instantaneously. On the contrary, due to the high viscosity of the liquid phase in heavy oil systems, gas will evolve from the liquid phase and exist as tiny bubbles initially. These small gas bubbles will coalesce, remain dispersed and gradually become a free gas phase to reach an equilibrium state (Lillico et al., 2001 and Uddin, 2005). The presence of gas bubbles in the liquid phase is referred to as foamy oil flow. "Foamy oil" phenomenon is an important recovery mechanism in the CHOPS process (Maini, 1999). Many experimental studies have shown that clusters of gas bubbles are distributed in a live oil system consisting of the dead heavy oil and solvent (e.g., methane or propane) (Treinen, RJ, et al., 1997 and Sahni, A, et al., 2001).

The diffusion rate of dissolved gas in the liquid (oil) phase plays an important role in the extent of foamy oil (i.e., the number and lifespan of bubbles formed) (Wieland and Kennedy, 1957 and Lillico et al., 2001). The evolved gas tends to coalesce with other nearby bubbles, rather than acting as a nucleation site to form new bubbles, if the diffusion rate is relatively high. On the other hand, the evolved gas would form many smaller bubbles if the diffusion rate is low (Uddin, 2005). The time it takes for the small gas bubbles to form large connected bubbles (at equilibrium) depends on several parameters, such as the diffusion rate of the bubbles, oil viscosity, interfacial properties (Ahmed et al., 1989; Batycky et al., 1997; Treinen et al., 1997 and Wong et al., 1999).

Foamy oil is highly relevant to CHOPS production because the viscosity of the foamy oil phase is much less than that of the equilibrium liquid phase. Smith (1988) described that the mobility of oil with dispersed gas bubbles could be increased significantly in comparison to the single-phase oil

mobility. The gas bubble growth process in a live heavy oil system is controlled by mass, momentum and the heat transfer across the gas-liquid interface (Theofanous et al., 1969; Szelely and Martins, 1971; Szelely and Fang, 1973 and Lillico et al., 2001).

It should be emphasized that foamy oil is essentially a non-equilibrium phenomenon; after sufficient time has elapsed, all bubbles would coalesce and a free gas phase would form at the equilibrium conditions. It is challenging to represent non-equilibrium phenomena directly in conventional reservoir simulators, which assume equilibrium conditions at each grid cell over a certain time step. Two main groups of approaches are commonly employed: modified equilibrium and kinetic models (Maini, 2001).

2.3.1.1 Modified Equilibrium Models

These models are relatively easy to implement in common compositional reservoir simulators, as they employ the typical assumption of complete local equilibrium between two immiscible phases. The non-equilibrium phenomenon is represented indirectly by modifying the fluid (PVT) model, multiphase flow functions (e.g., relative permeability), or viscosity models (Maini, 2001). Several of these equilibrium models, including the pseudo bubble point model, modified fractional-flow model, and reduced viscosity model, are described next.

In the pseudo bubble point approach, the bubble point pressure is an adjustable parameter in the fluid property description to model the foamy oil behavior. The solution gas remains in the oil phase until the reservoir pressure has dropped below the pseudo bubble point. Below the pseudo bubble point pressure, only a fraction of the released solution gas remains entrained. The entrained gas is treated as a part of oil phase. To mimic the delayed exsolution of gas, a lower bubble point pressure is assigned to suppress the dissolution of light components into the free gas phase, such

that the light components would remain in the oil phase and increase its mobility. In practice, a "pseudo-" bubble point pressure that is below is the true bubble point measured in a PVT cell at thermodynamic equilibrium conditions. This method can be readily implemented in most compositional reservoir simulators (Kraus et al, 1993). Indeed, the equilibrium ratios (K-values) are modified based on the pseudo-bubble point pressure in the model (Maini, 2001). The outcome of a pseudo bubble point is to suppress gas dissolution, which leads to lower gas-oil ratio (GOR) and sustained pressure maintenance, which are common characteristics associated with foamy oil flow (Maini, 2001).

In the modified fractional flow approach, the idea is to reduce the mobility of the free gas phase by modifying the gas relative permeability function with saturation. Lebel (1994) proposed a model, in which the evolved solution gas is entrained in the oil phase up to a certain system-dependent limiting volume fraction; consequently, no increase in free gas saturation is observable until the amount of evolved gas has finally exceeded that particular limit. The oil phase viscosity is kept low, as long as the light components would remain in the liquid phase. This approach requires the modification of the relative permeability functions (e.g., increasing the critical gas saturation and/or decreasing the gas phase relative permeability). Other similar approaches where the relative permeability functions are tuned to model the foamy oil flow were also proposed by Pooladi-Darvish et al (1999) and Firoozabadi et al (2001).

Reduced viscosity models were first introduced by Claridge and Prats (1995). The idea is that dispersed bubbles are stabilized due to the apparent adsorption of asphaltenes onto the bubble surfaces, and the net effect is a reduction in the viscosity of the oil phase. The coating of asphaltenes on the bubble surfaces helps to stabilize the small bubbles, enabling them to flow

through the porous medium within the oil phase, and significantly increases the oil phase mobility. However, this approach is not yet fully validated by experimental data (Maini, 2001).

2.3.1.2 Kinetic Models

The kinetic models capture the foamy oil behavior based on the non-equilibrium mass transfer approach (Uddin, 2005). The oil phase consists of three nonvolatile components: dead oil, dissolved gas, and dispersed gas bubbles. The conversions of dissolved gas to dispersed gas bubbles, as well as to the free gas phase, are formulated as a set of chemical reactions. Specific reaction parameters should be calibrated with experimental measurements.

This approach offers the advantage of capturing the dynamic bubble growth and nucleation processes in heavy oil systems. Therefore, in this thesis, the kinetic approach is used to model the foamy oil. More details are presented in Chapter 3.

2.4 Sand Failure Models

Quantifying the sand failure and production mechanisms in unconsolidated sandstone reservoirs is necessary for simulating the dynamic growth of wormholes during CHOPS. Field studies and laboratory experiments (Elkins et al., 1972; Yeung, 1995; Squires, 1993; Jensen, 1995; Geilikman and Dusseault, 1997 and Tremblay et al., 1998) corroborated the positive correlation between sand and oil productions. When an unconsolidated sandstone formation is subjected to pressure depletion, sand arches would form behind the perforation opening (Bratli and Risnes, 1981). Generally speaking, sand production is a result of the shear/tensile failure due to excessive fluid pressure drawdown in a poorly consolidated formation (Wang et al., 2005). The stresses distribution in the formation would depend on the principal in-situ stresses, the fluid pressure, flow

(drawdown) rate, the arch geometry, and the stress-strain relations of the sand (Bratli and Risnes, 1981). During CHOPS production, pressure depletion causes the sand failure at the tip of the arch (wormhole), which continues to propagate into the reservoir. A sand arch stability criterion was proposed by Bratli and Risnes (1981), who described the scenario where the sand surrounding the cavity was plastically deformed. It computes a critical pressure gradient, $\left(\frac{dp}{dr}\right)_{critical}$, which is the minimum threshold required at the tip of the arch for further failure; in other words, the sand arch would continue to grow, if the pressure gradient at the tip is greater than or equal to this critical value. It controls the extent of the wormhole propagation and subsequent sand production. This criterion is consistent with field observations for sand production in various North Sea fields.

$$\left(\frac{dp}{dr}\right)_{critical} = \frac{2C_u}{R_c} \tag{2-1}$$

Where C_u denotes the unconfined compressive strength and R_c is the average radius of curvature.

However, experimental studies seemed to suggest that the actual critical pressure gradient in CHOPS operations may be lower than the predicted value in **Equation 2-1**. Tremblay and Oldakowski (2002) performed a set of wormhole experiments with a sand pack (diameter: 29.8 cm; length: 80.4 cm) with the Clearwater sand collected from several cold production pilots. Two vertically aligned orifices of 1.27 cm in diameter were placed at the ends of the sand pack. A pressure depletion experiment was performed to simulate the production of oil, gas, and sand during CHOPS. A single sand-filled high porosity channel (36 cm in length by 17 cm in diameter) was observed starting from the orifice. The pressure gradient at the surface of the sand arches was approximately 7.1 - 7.5 MPa/m at 5.27 days when massive sand production had likely commenced; this value is much less than the critical pressure gradient of 15.4 MPa/m predicted according to

Equation 2-1. This reduction in the critical pressure gradient was attributed to the presence of foamy oil flow, and a factor, *f*, was added for CHOPS reservoirs (Tremblay et al., 2003):

$$\left(\frac{dp}{dr}\right)_{critical} = \frac{2fC_u}{R_c} \tag{2-2}$$

Other methods, such as the constitutive model for sand production proposed by Shao and Marchina (2002), did not invoke an explicit definition of sand arches or wormholes. Instead, the geomechanical response of an equivalent homogenized damage zone is modeled (**Figure 2-5**). The main drawback of this method is that the dynamic growth of individual wormholes cannot be depicted; only the incremental enhancement in the average permeability within the damaged zone is estimated.

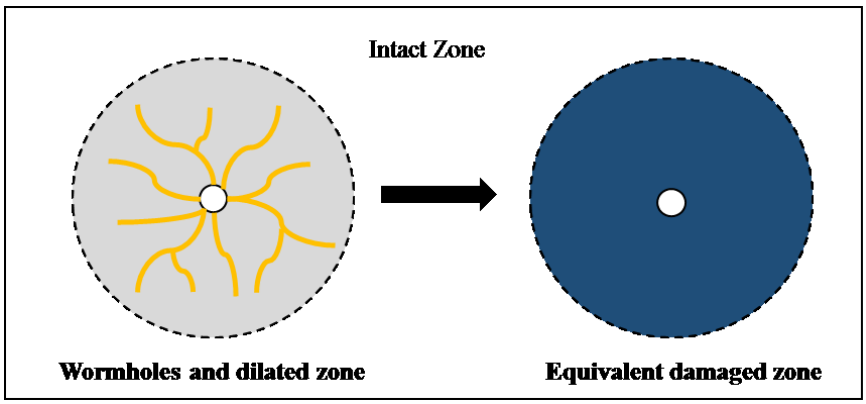

Figure 2-5: Wormhole represented by equivalent damaged zone (Modified from Shao and Marchina, 2002)

2.5 Numerical Simulation of CHOPS

Existing commercial simulation packages are not capable of incorporating the physical mechanisms described in section 2.2 without any modifications. In this section, previous works focusing on integrating sand production, wormhole growth, and fluid flow in simulation models are discussed.

Yuan et al (1999) described the wormhole growth process by the probabilistic active walker (PAW) approach. The PAW model consists of two parts: a potential function and a probability function. The potential function is derived from the pressure distribution, while the probability function is computed from the potential function, which determines the highest potential wormhole growth path. The ensuring growth pattern follows fractal statistics. Liu and Zhao (2005) proposed another wormhole growth model following the Diffusion-Limited Aggregation (DLA) algorithm, which is widely adopted to generate a broad variety of branching-growth fractal patterns encountered in many physical processes. An example is shown in **Figure 2-6**. The wormhole diameter distribution along throughout the network could be described using the Area Version of Gaussian Function (Liu and Zhao, 2005). The aforementioned models can be used to predict the potential wormhole pattern. In practice, sand production data should be history-matched to determine the possible lateral extent or range of the wormhole networks based on material balance calculations. Shokri and Babadagli (2012) utilized dual-permeability flow simulations to history match a set of DLA fractal patterns using sand production data collected during CHOPS. However, the drawback of their study is that the dynamic sand failure and wormhole growth processes were not represented, since a set of static fractal patterns generated using the DLA algorithm was employed.

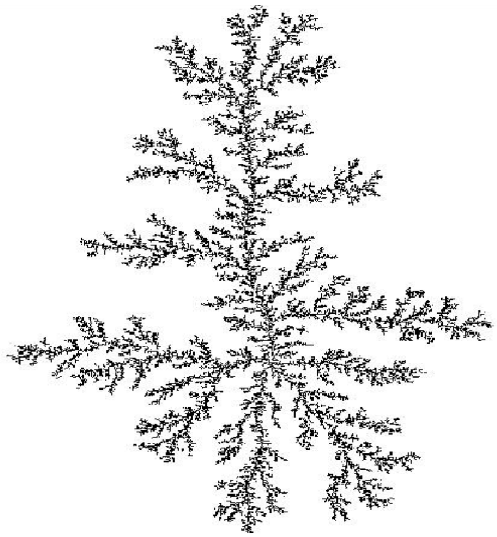

Figure 2-6: Example of a Wormhole Fractal Network

A dynamic wellbore CHOPS model was developed by Istchenko and Gates (2012), where the wormhole is represented as part of an extended wellbore. The growth of a particular wormhole is governed by the critical sand fluidization velocity, which is indirectly related to the critical pressure gradient in **Equations. 2-1 & 2-2**. The strengths of this model are that many of the main physical mechanisms, such as the foamy oil, sand failure, and sand production, are captured. It offers a simplified representation of the wormholes. However, the key limitation of this model is that the geomechanical criterion controlling sand failure cannot be explicitly integrated. Certain assumptions must be invoked to derive the critical sand fluidization velocity from the critical pressure gradient formulation.

Other studies aimed to capture the dynamic nature by assigning or defining a time-dependent region of enhanced permeability or conductivity. For example, Denbina et al. (2001) enhanced the transmissibility dynamically in the area surrounding the well to model the mechanism of wormhole growth and foamy oil. Cumulative field sand production was used to determine the radial extent

of the wormhole drainage zones. Sawatzky et al. (2002) at the Alberta Research Council (ARC) built a radial drainage model, where the wormhole zones were depicted as high-permeability regions. Their work resulted in a sand production module, which has since been coupled with a commercial reservoir simulator (namely CMG STARS). The module can predict the areal extent of a wormhole network and update the permeability distribution dynamically with a temporal enhancement. Within this module, the foamy oil behavior was modeled by reducing the gas phase relative permeability, in a fashion similar to the modified frictional-flow model (section 2.3.1.2). Their model was validated by history matching of oil/sand production data obtained from several CHOPS wells in the Edam field.

Finally, a multi-well CHOPS model was developed by Tremblay (2009) at the Saskatchewan Research Council (SRC) to simulate the connectivity and maximum diameter of a wormhole growth network involving multiple CHOPS wells. The SRC multi-well model was used initially to generate an equivalent representation of the wormhole network as a set of superposed multilateral wells. The multi-well model computes the times at which the wells are open and closed, the diameters of the equivalent multilateral wells, as well as the skin factors for individual multilateral wells (wormholes) associated with the enhanced permeability of the dilated sand around the open channel. The equivalent model can be subjected to flow simulation directly. Although the modeling procedure can simulate wormholes (as multilateral wells) dynamically, it cannot predict the actual growth paths of the wormhole network.

2.6 Gaps in Existing Numerical Studies

The literature review in the previous section examined various simulation approaches and studies pertinent to CHOPS analysis. In particular, various approaches were proposed to model the key physical mechanisms associated with CHOPS operations: foamy oil flow, sand failure, and wormhole growth. A key drawback in the existing simulation tools or methods is that the wormhole growth models are generally over-simplified. The dynamic processes of sand failure and wormhole growth are not fully represented. In some cases, field history was often employed to constrain the lateral extent of a static fractal pattern of wormhole network (Liu and Zhao, 2005). In other instances, wormholes are approximated as an extended wellbore (Tremblay 2009) or a radial region of enhanced permeability around the wellbore (Sawatzky et al., 2002). Numerous experimental studies in the past have revealed that sand failure is strongly influenced by foamy oil flow. Therefore, a robust simulation workflow that integrates the mechanisms of foamy oil flow, sand failure (governed by realistic geomechanical constraints) and fractal wormhole growth patterns is needed. An improved capability of modeling the realistic development or growth of wormholes during CHOPS is also key to assessing and modeling of post-CHOPS processes.

Chapter 3. Methodology

3.1 Overview

A geomechanically-constrained dynamic fractal wormhole growth model is proposed in order to simulate the CHOPS process. It offers an improvement to the commonly-adopted Diffusion Limited Aggregation (DLA) algorithm with a sand-arch-stability criterion. First, a computational mesh was constructed over a fractal pattern based on the Diffusion Limited Aggregation (DLA) algorithm in the reservoir simulator. Local grid refinement is implemented in the wormhole regions. Next, a new calculating procedure coupling compositional flow simulation with sand production is employed to compute the stability criterion for the sand arch (wormhole tip): the wormhole would continue to expand following the designated fractal pattern, provided that the pressure gradient at the wormhole tip exceeds the limit corresponding to a sand-arch-stability criterion.

3.2 Foamy Oil Model

As discussed in Chapter 2, the kinetic model can capture the dynamic time-dependent nature of foamy oil flow, without the assumption of pseudo-equilibrium between the free gas and oil phases. It can be readily incorporated in most commercial simulators as a set of pre-defined chemical

reactions. The kinetic foamy oil models proposed by Uddin (2005) was used to simulate the foamy oil behavior and documented in this thesis. The fomay oil kinetic model is implemented to simulate the dynamics of bubble nucleation and growth processes in a heavy oil reservoir. Five components are defined for the fluid model: water, dead oil, solution gas, dispersed gas bubble (oleic phase) and connected bubble (gaseous phase). The solution gas, dispersed gas bubble, and connected bubble are considered as pseudo components and exhibit the same chemical properties as methane (CH_4). It is contributed significantly to high oil phase compressibility. The keyword FREQFAC in CMG STARS (CMG 2016) is defined as the reaction frequency factor, which used to calculate the reaction rate. In this study, the transfer coefficients (reaction rate constants) presented in Uddin (2005) were applied in the base case model and tuned in the following history matches steps.

A kinetic model presented by Uddin (2005), which is based on a non-equilibrium mass transfer approach, is used to model the bubble nucleation and growth processes associated with foamy oil flow. In that model, the dispersed gas bubbles are assumed to flow in the oleic phase, when the bubble size is smaller than the pore throats in a given porous medium. As the bubbles aggregate and grow into larger bubbles (**Equation 3-1**) and exceed the pore throat diameter, the dispersed gas bubbles eventually become a continuous gaseous phase, (**Equation 3-2**). Indeed, since the dispersed gas bubbles have the same chemical properties as the solution gas (i.e., CH_4), the ensuing compressibility of the foamy oil phase is also high. The pseudo kinetic reactions are used to describe the physical processes of bubble nucleation and bubble growth:

Bubble Nucleation Processes:

$$\begin{cases} \text{Solution gas (G)} \rightarrow \text{Dispersed gas bubble (O)} \\ \text{Dispersed gas bubble (O)} + \text{Solution gas (G)} \rightarrow 2*\text{Dispersed gas bubble (O)} \end{cases} \quad (3\text{-}1)$$

Bubble Growth Processes:

$$\begin{cases} \text{Dispersed gas bubble (O)} \rightarrow \text{Connected bubble (G)} \\ \text{Dispersed gas bubble (O)} + \text{Solution gas (G)} \rightarrow \text{Solution gas (G)} + \text{Connected bubble (G)} \end{cases} \quad (3\text{-}2)$$

A schematic of the bubble nucleation and bubble growth processes in foamy oil is shown in **Figure 3-1**.

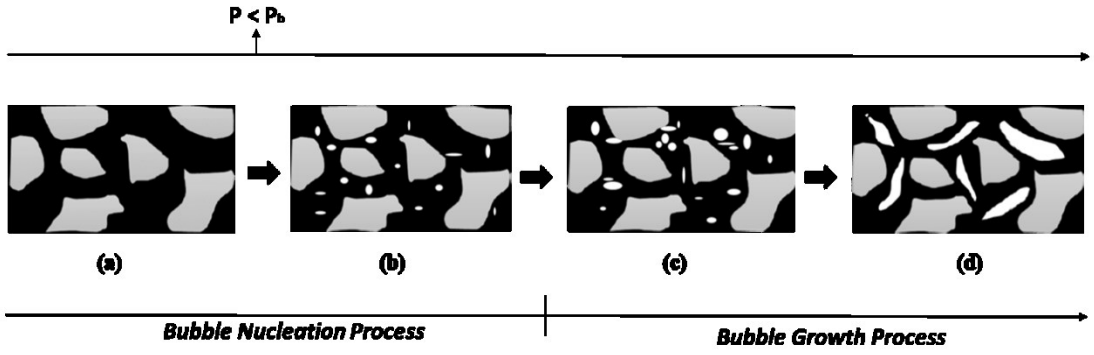

Figure 3-1: A schematic of the foamy oil bubble nucleation and bubble growth physical process: (a) Solution gas; (b) Dispersed gas bubble; (c) Connected bubble; (d) Formation of a continuous gas phase

These pseudo kinetic reactions can be implemented into the compositional reservoir simulator using the following chemical reaction equations. Specifically, the mass transfer rates for the above kinetic reactions can be defined as:

$$r_d^1 = N_1\left(C_{gd} - C_{gd}^{'}\right) \quad (3\text{-}3)$$

$$r_d^2 = N_2(C_{gd} - C_{gd}^{'})^2(C_{bd}) \quad (3\text{-}4)$$

$$r_c^1 = G_1\left(C_{bd}\right) \quad (3\text{-}5)$$

$$r_c^2 = G_2(C_{gd} - C_{gd}^{'})^2\left(C_{bd}\right) \quad (3\text{-}6)$$

Where r_d^1 and r_d^2 are the transfer rates of solution gas into dispersed gas bubbles (**Equation. 3-1**), and N_1, N_2, G_1 and G_2 are the transfer coefficients for the above kinetic reactions (**Equations 3-3 to 3-6**); C_{gd} and C_{bd} refer to the actual molar concentrations of solution gas and dispersed gas bubbles, respectively, C'_{gd} is the equilibrium dissolved gas concentration. r_c^1 and r_c^2 are the transfer rates of dispersed gas bubbles into connected bubbles (**Equation 3-2**). In addition, the C_{gd} is defined as $C_{gd} = (\phi S_o \rho_o)(x_{gd})$, where ϕ is the porosity, S_o is the oil saturation, ρ_o is the oil phase mole density, and x_{gd} is the dissolved gas mole fraction. Similarly, the C'_{gd} is defined as $C'_{gd} = (\phi S_o \rho_o)(x'_{gd})$, where x'_{gd} is the equilibrium dissolved gas mole fraction in oil phase, which is determined by its the pressure dependent K-values and the gas mole fraction or equation of state.

In most practical applications, these transfer coefficients (N_1, N_2, G_1 and G_2) are calibrated against laboratory data. For example, in Uddin (2005), gas exsolution and pressure depletion data obtained from a series of mercury withdrawal experiments to calibrate the foamy oil kinetic parameters, as implemented in STARS. The same coefficients are also used in this study, due to a lack of additional laboratory data. In the field case example in Chapter 4, these coefficients are slightly adjusted to achieve a better match with the production history.

The oil (liquid) phase viscosity is estimated using the phase mixing rules:

$$\ln(\mu_o) = \Sigma_i [f_{oi} * \ln(\mu_{oi})] \tag{3-7}$$

where μ_o is the oil (liquid) phase viscosity, μ_{oi} is the viscosity of component *i* in the liquid phase, and the f_{oi} is the weighting factor corresponding to component *i*.

In CMG STARS™, the equilibrium *K* values are correlated by the **Equation 3-8**:

$$K(P,T) = (\frac{kv_1}{P} + kv_2 * p + kv_3) * e^{\frac{kv4}{T - kv5}} \quad (3\text{-}8)$$

where P is the pressure (kPa), T is the temperature (°C) and kv_1, kv_2, kv_3, kv_4 and kv_5 is the coefficients in the correlation for K values for specific gases.

3.3 Sand Failure Criterion

In the unconsolidated sandstone reservoirs (such as those encountered in CHOPS), stable sand structures (sand arches) may form around the wellbore or over a perforation due to shear failure or hydrodynamic forces during pressure depletion. Progressive destabilization of sand arches would create a wormhole network that continues to grow away from the wellbore or perforation (Sawatzky et al., 2002). The shear failure of sand is governed by the Mohr-Coulomb criterion. Therefore, geomechanical constraints must be considered when modeling wormhole growth during CHOPS.

The existing tip of a wormhole is represented by a sand arch; the wormhole would continue to grow, provided that the pressure gradient at its tip exceeds the limit corresponding to a sand-arch-stability criterion. This sand-arch-stability criterion is defined by a critical radial pressure gradient, which is derived from the classical theory for sand arch failure under loading due to fluid flow (Bratli and Risnses 1981):

$$\left(\frac{dp}{dr}\right)_{critical} = \frac{2fC_u}{R_c} \quad (3\text{-}9)$$

Where C_u is the unconfined compressive strength, R_c is the average radius of curvature for the sand arch, and f is constant. In Bratli and Risnses (1998), f is equal to 1; however, measurements of the critical pressure gradient in the wormhole growth experiments using live heavy oil samples conducted by Tremblay and Oldakowski (2003) would suggest a much smaller value of f. They explained that the destabilizing effects of gas exsolution from the live oil and foamy oil flow corresponding to the pressure dropdown near the wormhole tip may lead to a lower critical pressure gradient. **Equation 3-10** is used to compute the average radius of curvature:

$$R_c = \frac{x_{\max}^{\ 2}}{z_{\max}} \tag{3-10}$$

The above equation conceptualizes the wormhole as an ellipsoid, where z_{max} is the major axis of the ellipsoid (wormhole length/2) and x_{max} is the minor axis of the ellipsoid (wormhole diameter/2).

When modeling the wormhole growth, only the sand-arch stability at the tip is considered, while the diameter of the wormhole is kept constant. Experiments conducted using sandpacks by the Alberta Research Council confirmed that the diameter of the wormhole would remain approximately constant, even though a portion of the loose sand within the wormhole was soured away. (Tremblay et al., 1996; 1997; 1998; 1999). In addition, it has been concluded that much of the oil flow happens at the tip of the wormhole, indicating that the wormhole growth is fastest at its tip, and the rate of wormhole growth should be proportional to the oil rate. The higher the flow rate, the higher the pressure drop across the wormhole tip, which is more likely to exceed to a critical threshold in **Equation 3-9**.

While the critical pressure gradient is defined based on the sand-arch-stability criterion (**Equation. 3-9**), the value of *f* should be determined via experimental measurements or tuned via history matching of the sand production data. It is assumed in this study that the wormhole diameter is 50 cm, which is consistent with field observations reported in Chang and Ivory (2013). The unconfined compressive strength of unconsolidated sand can be estimated from petrophysical and geomechanical measurements including rock elastic moduli (Young's modulus and shear modulus), porosity, and other formation properties (Chang et al., 2006). Unconsolidated sand formations in the Lloydminster heavy oil reservoirs are relatively weak, and the range of 5-20 kPa for the unconfined compressive strength of the sand has been reported in the literature (Tremblay et al., 1997; 1998; 1999).

The wormhole locations are updated dynamically in the simulation grid. Once it is determined that the tip would grow in a particular direction, the nearby cell is converted from a matrix block to a wormhole block: the sand is "removed", causing the porosity and permeability to correspondingly increase. Several experiments involving X-Ray Computed Tomography conducted by the Alberta Research Council showed that the porosity inside a wormhole is approximately 53% (Tremblay et al., 1996).

3.4 Sand Production Model

Sand production in CHOPS is the result of two sources: 1) propagation of the high-permeability wormhole network, in accordance to the sand-arch-stability criterion; 2) scouring of sand that has settled in the existing high-permeability channels within the wormhole network. The first source is the primary contributor, and its role has been corroborated extensively by field observation,

when much of the sand production is recorded within the first four months of production (Haddad and Gates, 2015).

The kinetics-based fluidization model is used to model the sand production in the numerical simulator. The formulation resembles that of the foamy oil and can be readily implemented in a similar fashion (CMG, 2016). The kinetic reaction describes the fluidization of settled sand in the solid phase to mobile sand in the oil phase.

$$Sand_{solid\ phase} \rightarrow Mobile\ Sand_{oil\ phase} \tag{3-11}$$

The corresponding equation to calculate the rate of mass transfer shown in the **Equation 3-12**.

$$\text{Reaction Rate} = \begin{pmatrix} \left(\frac{V - V_{crit}}{Vref}\right)^{\exp} & \text{when } V > V_{crit} \\ 0 & \text{otherwise} \end{pmatrix} \tag{3-12}$$

where V_{crit} is the critical oil phase velocity, V is the oil phase velocity, and V_{ref} is the reference velocity for reaction rate. The reaction rate depends on the critical oil phase velocity (V_{crit}) and the reference velocity for the reaction rate (V_{ref}). The exp represents the exponent in velocity factor that defines as a non-zero value in this reaction equation. If the history of sand production data is available, they can be used to tune these parameters in a history matching procedure. Inside a wormhole cell, the value of V is high; hence, the rate of sand production is also high, in comparison to an intact matrix cell. It should be noted that sand production data are not recorded consistently and reliably in most cases; in addition, only cumulative sand production volumes may be reported monthly.

3.5 Diffusion Limited Aggregation (DLA) Algorithm

As in most cases in subsurface reservoir modeling, it is nearly impossible to precisely delineate a single deterministic wormhole network configuration. Many of the previous studies, such as Liu and Zhao (2005), proposed that wormhole growth could be described by fractal statistics, and the Diffusion Limited Aggregation (DLA) model, which simulates the fractal branching process, can be employed. The DLA method was first introduced by Witten and Sander (Witten and Sander, 1981; Feder, 1988) to describe irreversible growth phenomena. It describes how particles that are undergoing random walks due to the Brownian motion (diffusion) may aggregate to form clusters. The resultant cluster patterns are fractals. This method and has been successfully applied to simulate many phenomena, such as Hele-Shaw flow (Meakin, 1988), mineral deposits, electrodeposition, growth of bacterial cell colonies and dielectric breakdown. Branching patterns are also common phenomena in geology and geophysics, such as fracture patterns and makings on joint surfaces in structural geology, viscous gingering fronts in petroleum and river networks in geomorphology.

Figure 3-2 illustrates four different realizations of fractal patterns generated by the DLA model, in which the fractal dimension is kept consistent.

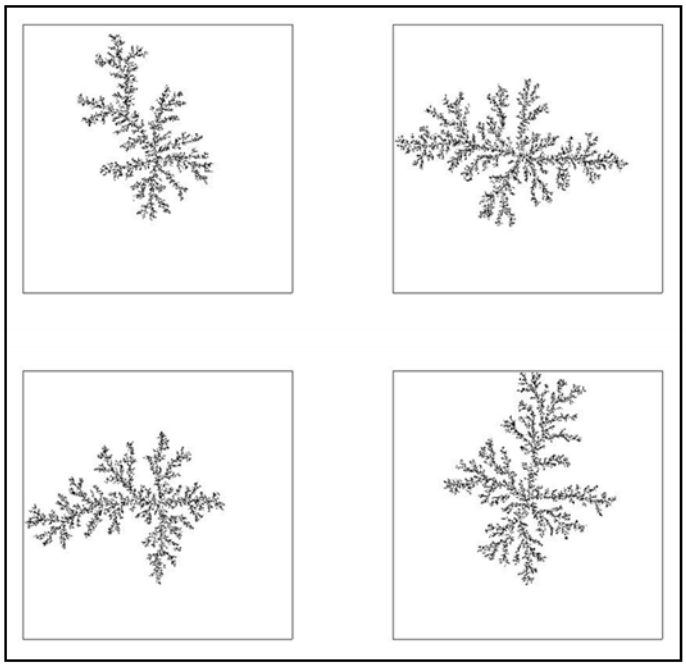

Figure 3-2: Multiple realizations of fractal patterns generated by DLA model

In summary, the DLA model can be used to simulate random growth processes, where the growth probabilities at the surface of the growing structure are proportional to the gradient of a scalar field that obeys the Laplace equation. It means that if a randomly branched pattern is observed and if a scalar field $\Phi(\mathbf{r})$ obeying the Laplace equation (**Equation 3-13**) can be associated with the physical process controlling that pattern formation, then the ensuing pattern is likely to be represented by the DLA model:

$$\nabla^2\Phi = 0 \tag{3-13}$$

$\Phi(\mathbf{r}) = 0$ at all positions $\mathbf{r}$ occupied by the cluster, and $\Phi(\mathbf{r}) = 1$ (or some other constant value) for $|\mathbf{r}| = \infty$. In the DLA model, the probability **P(r)** that a random walk will visit the lattice site at position $\mathbf{r}$ is proportional to $\Phi(\mathbf{r})$. For instance, the discretized Laplace equation is shown in **Equation 3-14**.

$$\Phi(i,j)=\frac{1}{4}\left[\Phi(i-1,j)+\Phi(i+1,j)+\Phi(i,j-1)+\Phi(i,j+1)\right] \tag{3-14}$$

The corresponding probability that a random walk will reach the lattice site (*i, j*) are related to the probabilities of visiting the neighboring sites.

$$P(i,j)=\frac{1}{4}\left[P(i-1,j)+P(i+1,j)+P(i,j-1)+P(i,j+1)\right] \tag{3-15}$$

where $\Phi(i, j)$ is the scalar potential associated with the site at position (*i, j*) on a 2D square lattice, and $P(i, j)$ is the probability that a random walk would visit that particular lattice site.

For CHOPS, wormhole development in unconsolidated sandstones is governed by the pressure field, and pressure diffusion obeys the Laplace equation approximately, enabling the growth of wormhole to be modeled by the DLA model (Liu & Zhao, 2005). Selinger et al (1989) proposed a generalized DLA model to model viscous fingering in a porous medium with heterogeneous permeability and homogeneous porosity, where the transition probabilities would depend on the local permeability (Selinger et al., 1989). The DLA model has been employed in the past to simulate anisotropic wormhole growth in the CHOPS heterogeneous reservoirs by assigning different probabilities for different directions (Liu & Zhao, 2005).

In this study, a single well case was performed to simulate the CHOPS process. It is assumed that the well is located on the geometrical center of the model and the fractal pattern would grow away from the wellbore. As discussed previously, the wormhole diameter is set to 50 cm, which is consistent with field observations in Chang and Ivory (2013). Following the DLA algorithm, several realizations of 2D fractal wormhole patterns are generated (Figure 3-2). Each realization is binarized: blocks with a value of 1 represent the presence of wormholes, while blocks with a

value of 0 belong to the matrix (Figure 3-3). The mesh is locally refined surrounding the wormhole regions (Figure 3-4).

0	0	0	0	0	0	0	1	0	0	0	0	0	0	0
0	0	0	0	0	1	0	1	0	0	0	0	0	0	0
0	0	0	0	0	1	1	1	1	0	0	0	0	1	0
0	1	0	0	1	1	0	0	0	0	0	0	1	1	1
1	1	1	0	0	1	1	0	1	0	1	0	1	0	0
0	0	1	0	0	0	1	1	1	0	1	1	1	0	0
0	1	1	0	0	1	0	1	0	0	0	1	0	0	0
0	0	1	1	1	1	1	1	1	1	1	1	1	1	0
0	0	0	1	0	1	0	1	1	1	0	0	1	0	0
0	0	0	0	0	0	0	1	0	0	0	0	1	0	0
0	0	0	0	1	1	1	1	1	1	1	1	0	0	0
0	0	0	1	1	0	0	1	1	0	0	1	1	0	0
0	0	1	1	0	0	0	0	1	1	0	0	1	1	0
0	0	0	0	0	0	0	0	1	0	0	0	0	0	0
0	0	0	0	0	0	1	1	1	0	0	0	0	0	0

Figure 3-3: Binary representation of wormhole networks

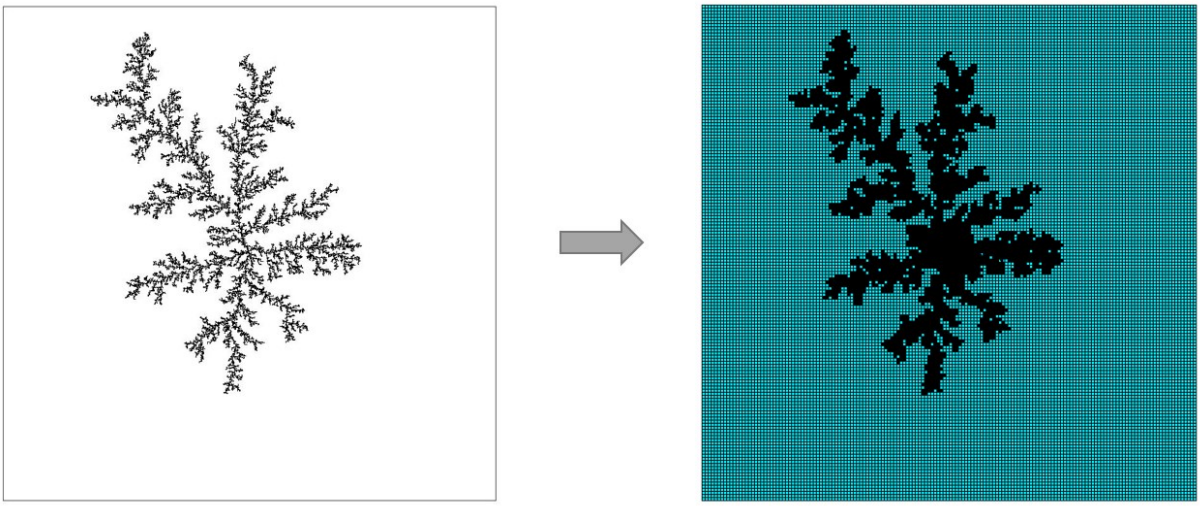

Figure 3-4: A realistic fractal wormhole pattern that introduced to geological model

3.6 Dynamic Fractal Wormhole Growth Workflow

In this research, a novel workflow that integrates compositional flow simulation, sand failure, and fluidization, as controlled by the sand-arch-stability criterion and fractal growth pattern, is formulated and implemented to model the CHOPS.

A flow chart of the general coupling strategy is shown in **Figure 3-5**. Two key steps are introduced:

1. Extract the pressure values at the wormhole tips.
2. Determine the wormhole growth direction (if any). Wormhole permeability is updated (i.e., increased), while wormhole porosity will be updated gradually by the sand fluidization model, which depends on the oil phase velocity.

These steps are implemented in Matlab (Mathworks, 2017a) and coupled with the numerical reservoir simulator (CMG-STARS 2016).

To control the wormhole growth dynamically, the sand-arch-stability criterion is used to determine whether the existing wormhole should continue expanding along the prescribed statistical fractal pattern. At the end of the flow simulation step, the flow simulation is paused temporarily, such that the Matlab code would read in the results file and extracts the computed pressure field. Next, it computes the pressure gradient at the tip of each existed wormhole. If the sand-arch-stability criterion is met, the wormhole would continue its growth along the direction prescribed by the fractal pattern. Otherwise, the production would continue with the existing wormholes.

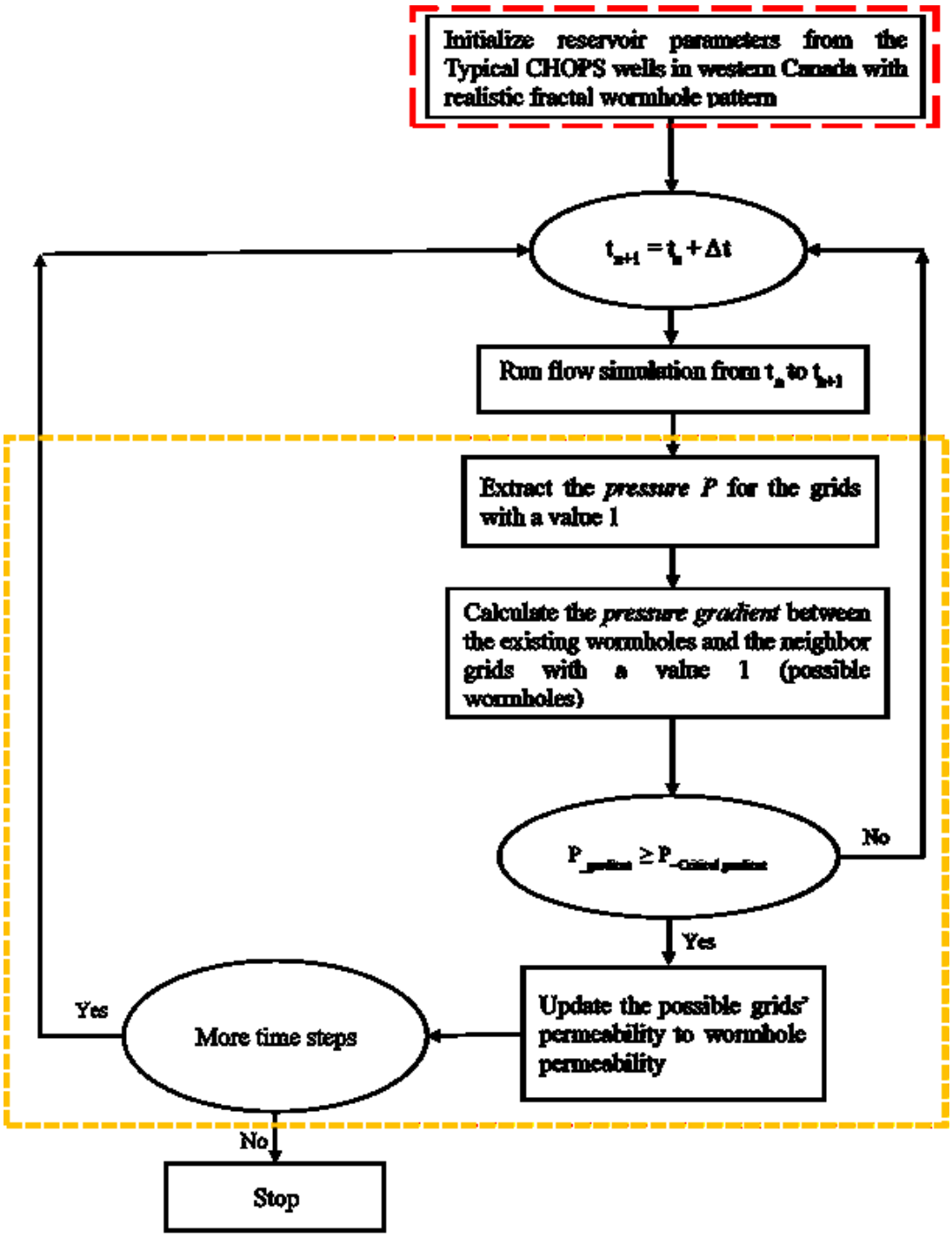

Figure 3-5: Flow chart for dynamic wormhole growth workflow

An example illustrating the wormhole development over several time steps is shown is presented in **Figure 3-6**. For the Cartesian grid system, each cell is surrounded by 4 neighbors, so the wormhole growth direction can be identified by inspecting the neighboring blocks with binary wormhole indices of 1 in that four direction (i.e., $i\pm1$ and $j\pm1$). For example, in **Figure 3-6-I**, for the wormhole to grow way from the wellbore after the first time step, the pressure gradients between the well block and its east, south, and west neighbors are computed. If the sand-arch stability criterion is satisfied, the wormhole is extended in that direction: the permeability and porosity of the neighboring block are updated, as discussed in the previous section.

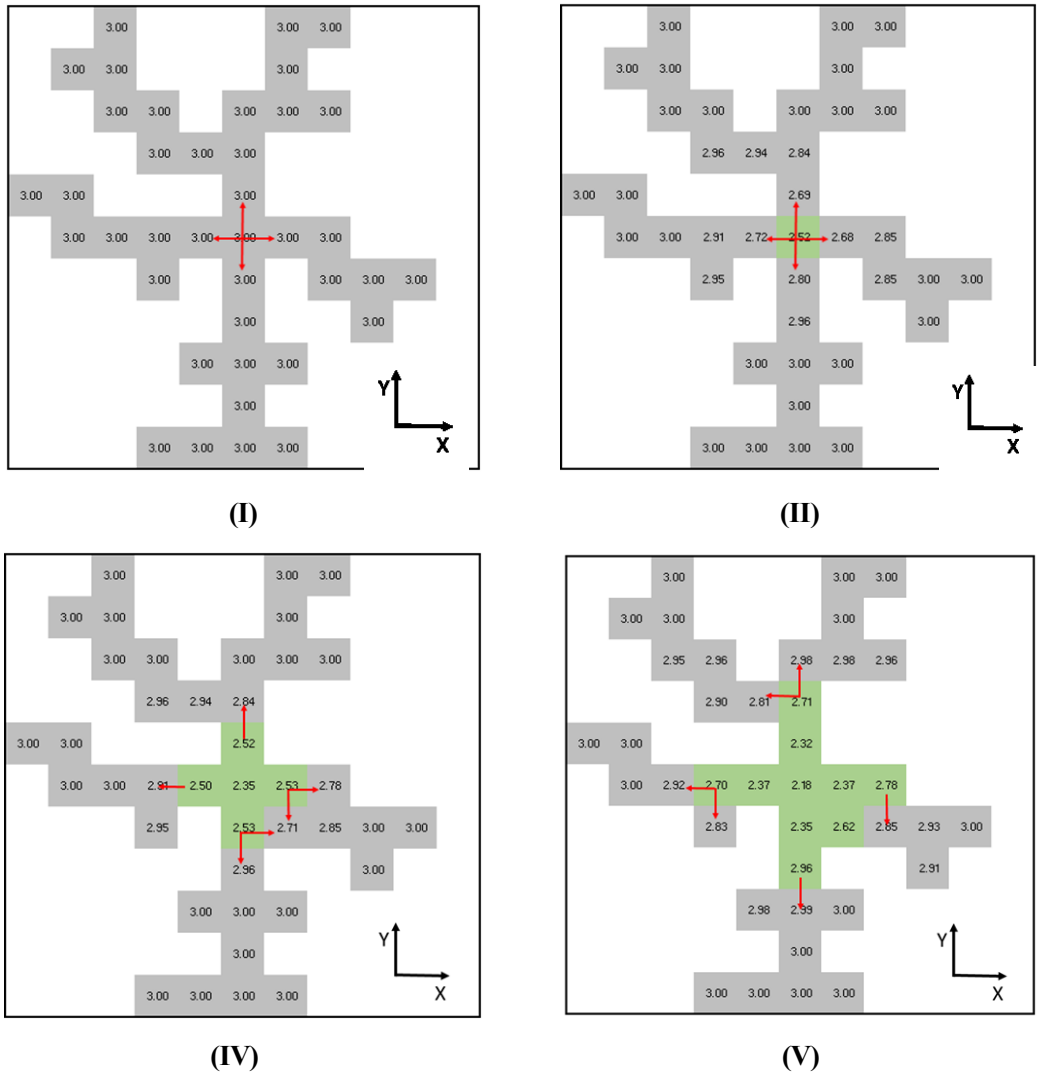

Figure 3-6: A simple prescribed fractal wormhole introduced to 2-D geological model at different time states. A producer well located in center of grid block. The grey color represents potential presence of wormhole while the white color belongs matrix; the number insides of the cell represents the reservoir pressure at initial state. The red arrow represents the search algorithm, which only followed the prescribed statistical fractal pattern. (I – represents at the initial state; II – represents the after first time period state; IV – represents the after second time period state and V – represents after the third time state)

Chapter 4. Field Case Study

4.1 Overview

In the previous chapter, a novel simulation workflow was introduced to model the CHOPS process. Specifically, the dynamic growth of a wormhole network is based on both realistic fractal statistics and appropriate geo-mechanical constraints associated with sand failure. In this chapter, the workflow is implemented to model a typical field-scale CHOPS reservoir, where the data was assembled from the public domain. The results are analyzed and compared to those presented in other studies in the literature. Sensitivity of the wormhole growth pattern and the ensuing CHOPS performance due to various system variables is also examined.

4.2 Model Setup

A typical CHOPS well from the Cold Lake heavy oil field in the Lloydminster area of Alberta, Canada is constructed. The production data and other relevant parameters are extracted from other studies in the literature (Sawatzky et al., 2002; Istchenko and Gates, 2002).

A single well is modeled and placed in the center of the computational domain. It is assumed that the wellbore is connected to the reservoir through the wormhole network. In addition, the wormhole is propagating only laterally (or horizontally), and expansion along the vertical direction is ignored. The rationale is that for most heavy oil reservoirs in Western Canada that are exploited by CHOPS, the deposition depth is generally greater than 350 m, where the vertical stress is much

greater than horizontal stress. In addition, thin pay thickness, coupled with high oil viscosity, would result in negligible vertical pressure drop. Hence, sand failure along the horizontal direction is more dominant.

4.2.1 Simulation Grid

Given that the vertical wormhole growth is neglected, a 2D reservoir model is constructed. The model parameters are extracted from Sawatzky et al. (2002) and Istchenko and Gates (2002), and they are summarized in **Table 4-1**. The model is 400 m × 400 m along the *x*- and *y*-directions, respectively ($\Delta x = \Delta y = 2.5$ m). The total reservoir thickness is 6.5 m, and the wormhole growth is limited to the middle layer of 3.5 m in thickness. The simulation domain is discretized into 160 × 160 × 3 grid blocks, and it is further refined locally in the wormhole regions ($\Delta x = \Delta y = 0.5$ m, which is consistent with the experimental observation of a typical wormhole's diameter). One producing well is placed at the center of the model, as shown in **Figure 4-1**. The wormhole porosity is defined as 0.52, in accordance to the experimental observations by Tremblay (2002). Meanwhile, the wormhole permeability in this study is adjusted as a history matching parameter.

Table 4-1: Parameters used in numerical model

Property	**Values**
Model size, m	400*400*6.5
Number of grids	160*160*3
Grid cell sizes ($\Delta x*\Delta y*\Delta z$), m	Top layer: 2.5*2.5* 1.5 Middle layer: 2.5*2.5*3.5 Bottom layer: 2.5*2.5 *1.5
Depth, mTVD	423.5
Pay thickness, m	3.5
Average porosity, fraction	0.34
Average vertical permeability, D	3
Average horizontal permeability, D	3
Average wormhole porosity, fraction	0.52
Average wormhole permeability, D	26350
Oil saturation	0.72
Dead oil viscosity, cP	20788 @ 20 ^{O}C
Solution Gas-Oil Ratio, m^3/m^3	10 @ 3000 kPa
Mole fraction of CH_4 at initial reservoir conditions (x_i)	0.149
Initial Reservoir Pressure, kPa	3000
Oil-Water Relative Permeability Curves Endpoints	Krocw = 0.48; Krwiro = 0.8 Swcrit = 0.2; Sorw = 0.2
Critical Pressure Gradient, kPa/m	66.8
Bottom Hole Pressure, kPa	500
Formation Compressibility, 1/kPa	$2.9*10^{-6}$ @ P_{ref} = 100 kPa

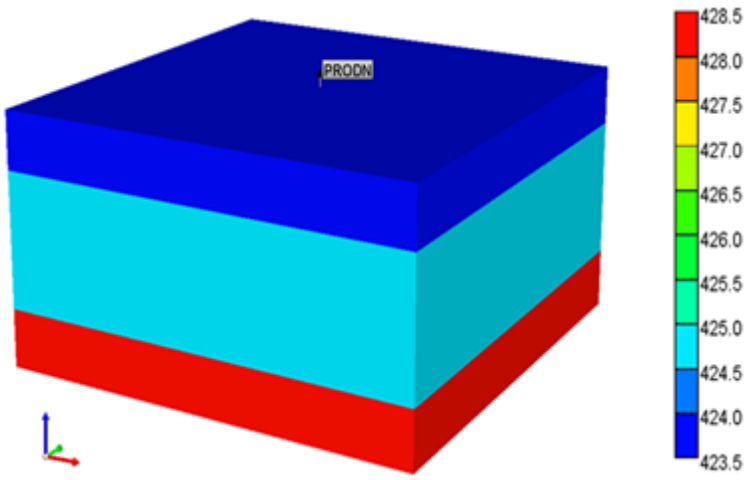

Figure 4-1: Single-well reservoir model (160x160x3) for CHOPS well

4.2.2 Reservoir Fluid Model

No detailed fluid analysis for this particular CHOPS well was available in the literature; therefore, the fluid properties for several typical CHOPS wells from Lloydminster area, as presented in Chang et al. (2015), is adopted here. The k_v values used in the simulation model are listed in **Table 4-2**. K value for oil phase component is zero. Two components are modeled: dead oil and methane (**Table 4-3**). Live oil at reservoir conditions is represented by the solution of methane into the dead oil. To simulate the effect of gas mobility reduction, relative permeability to gas is interpolated based on the amount of the free gas component. Two sets of relative permeability functions, as presented in **Figure 4-2,** are used: Set #1 is used when the mole fraction of "solution gas" is greater 0.8, while Set #2 is used when the mole fraction of "solution gas" is less than 0.3. The relative permeability functions are interpolated between the two sets, if the mole fraction of "solution gas" is between 0.3 and 0.8. Set #1 corresponds to the scenario with little free gas (hence the reduced gas mobility), while Set #2 corresponds to the scenario with much free gas.

Non-equilibrium foamy oil reaction parameters (as defined in **Equations 3-3** to **3-5**) are N_1 = 1.1 1/day, N_2 = 0.3542 (gmole/m^3)$^{-2}$/day, G_1 = 0 1/day and G_2 = 0.13 (gmole/m^3)$^{-2}$/day, respectively. The bubble properties are assigned to be identical to those of methane.

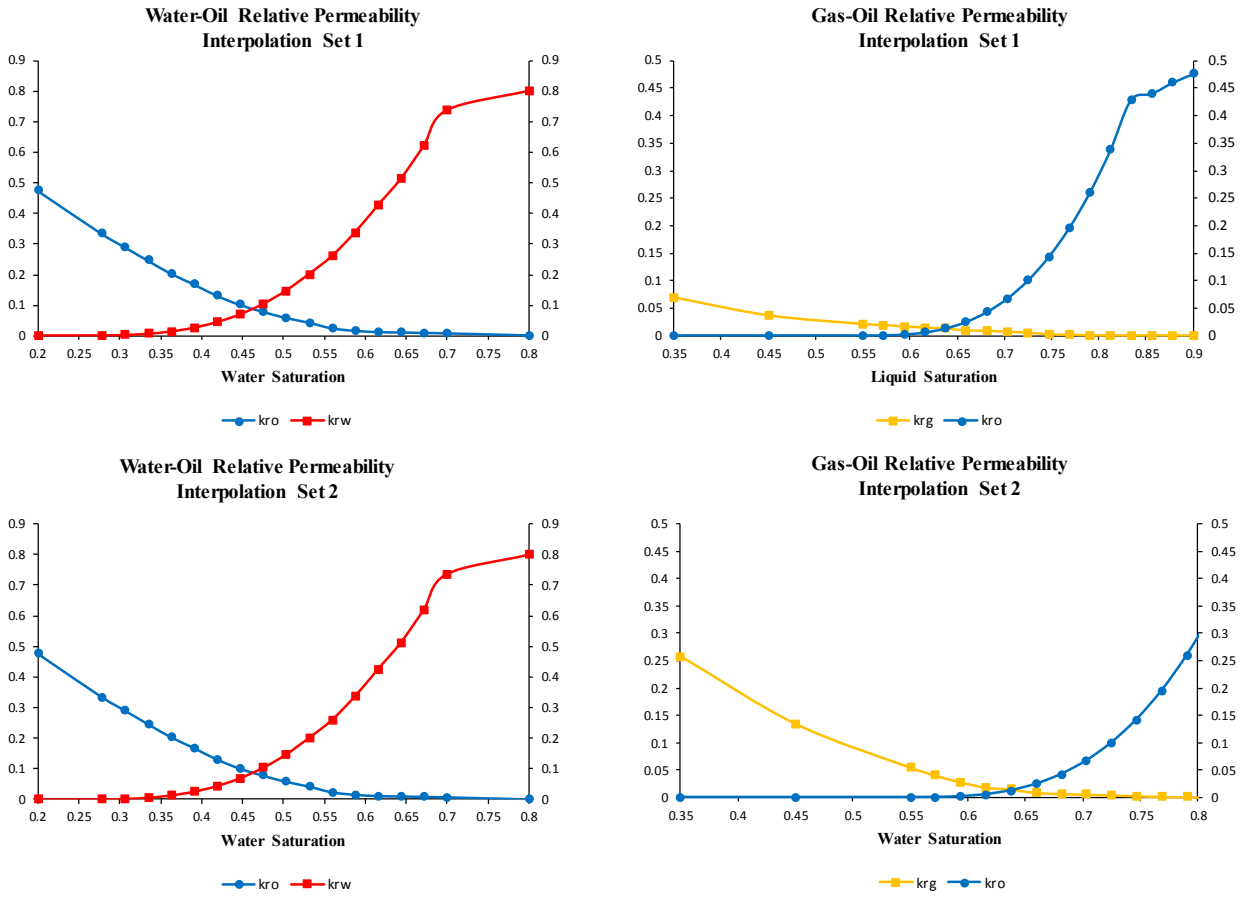

Figure 4-2: Two sets of Relative permeability functions

Table 4-2: Solution gas K_v values at 20 °C

Pressure (kPa)	Solution gas (CH_4)
200	109.9
1000	22.0
2000	11.0
3000	7.3

Table 4-3: Fluid proprieties for foamy oil flow model

Component Name	Dead oil	Solution gas (CH_4)	Dispersed gas bubble	Connected gas bubble	Large gas bubble
Molecular weight, g/gmole	511	16	16	16	16
Specific gravity	0.98	0.3	Gassy liquid	Gas	Gassy Solid
Compressibility, kPa^{-1}	$1x10^{-6}$	$7.5x10^{-6}$	Gassy liquid	Gas	Gassy Solid
Pc, kPa	1,158	4600	4600	4600	4600
Tc, °C	913.46	-82.5	-82.5	-82.5	-82.5
Molar density, mol/cm^3	1917.8	$1.875x10^{-4}$	41.8	Gas	41.8

4.2.3 Prescribed Wormhole Fractal Pattern & Sand Failure Model

A randomly selected DLA fractal pattern, as shown in **Figure 4-3**, was introduced with locally-refined grids to the geological model as the prescribed statistical fractal pattern.

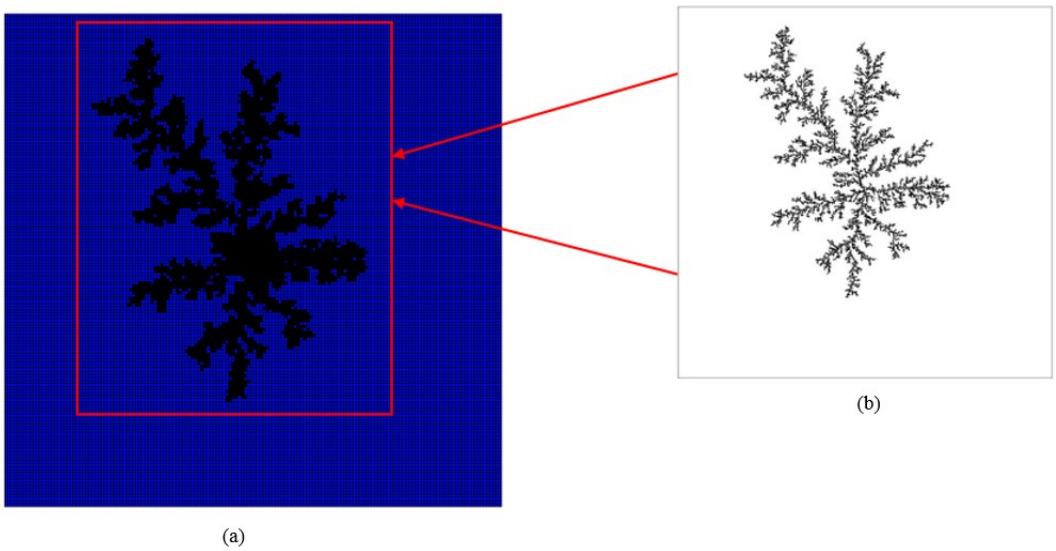

Figure 4-3: A selected fractal wormhole pattern applied on the geological model with locally-refined grid ((a). Geological model with applied prescribed statistical fractal pattern (b). A random selected DLA fractal pattern)

As discussed in section 3.4, a sand failure criterion based on geo-mechanical constraints is defined to dynamically control the growth of a fractal wormhole pattern. The compressive strength (*UCS*) is correlated to porosity:

$$UCS = a + b/(\phi - c) \tag{4-1}$$

where *UCS* is the unconfined compressive strength, kPa; a, b and c are experimentally determined (empirical) constants; ϕ is defined as the reservoir porosity.

For a typical CHOPS well, values presented by Chang et al. (2015) are used:

$$UCS = 12.78 + 1.01/(\phi - 0.291) \tag{4-2}$$

Using an average porosity of 0.34, the *UCS* value is approximated as 33.4 kPa according to **Equation 4-2**. For a wormhole diameter of 0.5 m (50 cm), the average radius of curvature for the sand arch is calculated to 1 m based on **Equation 3-10**. The constant f (≤ 1) in **Equation 3-9** is adjusted as a tuning parameter via history matching of the field data to model the influence of foamy oil flow. In the end, the critical pressure gradient corresponding to the wormhole growth is set as 66.8 kPa/m in our base model where f assumed equals 1.

The production data corresponding to an actual CHOPS well, including oil production rate, water production rate, and cumulative sand production, are extracted from Istchenko and Gates (2012). Given that an arbitrary fractal pattern is selected, certain parameters such as f, wormhole permeability, and the foamy oil kinetic reaction parameters, are chosen as tuning parameters when history matching the production data. The model predictions obtained from the proposed workflow will also be compared against other alternative approaches, such as the extended wellbore method presented by Istchenko and Gates (2012).

4.3 Results and Discussion

4.3.1 Base Case Study

At the initial state, there are zero wormholes in the model. As the pressure declines during production, the wormhole may grow along following a certain fractal pattern, provided that the pressure gradient at the wormhole tips smaller than the critical pressure gradient. As explained in Chapter 3, the fractal pattern has been coded with a set of binary indices (0 – no wormholes, 1 – wormholes). Therefore, at the end of each time step, the potential growth direction is identified by selecting the neighboring blocks with an index of 1. If the pressure gradient between the existing wormhole grid block and its neighbor is greater than the critical pressure gradient, the wormhole will expand in that direction, and the wormhole network is updated dynamically along that particular direction. After history matching, a critical pressure gradient of 50.06 kPa/m corresponding to the f of 0.75 is obtained.

As wormholes propagate in the reservoir, the porosity/permeability in the wormhole channels are updated accordingly. **Figures 4-4** shows the top view of the middle layer with wormhole propagating away from the wellbore. The simulation predictions of monthly oil production rate and the cumulative sand production are compared to the actual field histories in the **Figures 4-5**.

After the first 3 months of producing period, the wormholes start to grow around the wellbore quickly, leading to an enhanced oil production rate. During the initial production stage, there is a significant pressure drawdown in the near wellbore region, causing the unconsolidated sandstone to fail and creating these high permeability channels around the wellbore. During the production period from 5 to 12 months, there is little change in the wormhole network. During this later stage of production, souring of the sand production process tends to dominate, and the pressure gradients

at the wormhole tips are generally insufficient to erode the sand matrix any further. It is also evidenced by the reduction in produced sand volume in comparison to the initial 3 months. As the production continues, the pressure gradient may continually increase at the wormhole tip, and in that case, the wormhole growth will again after certain duration of time.

It is also interesting to note from **Figure 4-4** that the intensity of the wormhole network decreases as the distance from the wellbore increases. In other words, the wormholes become more sparsely populated as they advance further into the reservoir. It is consistent with the experimental observations conducted by Tremblay et al. (1997). Mathematically, it is represented via the fractal statistics in the wormhole patterns. Physically, it is the result of a drastic decline in the pressure gradient at the wormhole tip, as it propagates into the reservoir; there is less driving force for flow (smaller pressure drops) as the distance from the wellbore. **Figures 4-5** shows the top view of the pressure distribution in the wormhole layer (mid-layer) over the first 12 months. Much of the pressure drop is observed during the initial 3 months of production, and this is corroborated by the wormhole distribution in **Figures 4-4**. As the wormholes propagate further into the reservoir, sand and fluids (oil and gas) would flow through the high conductivity channel to the wellbore.

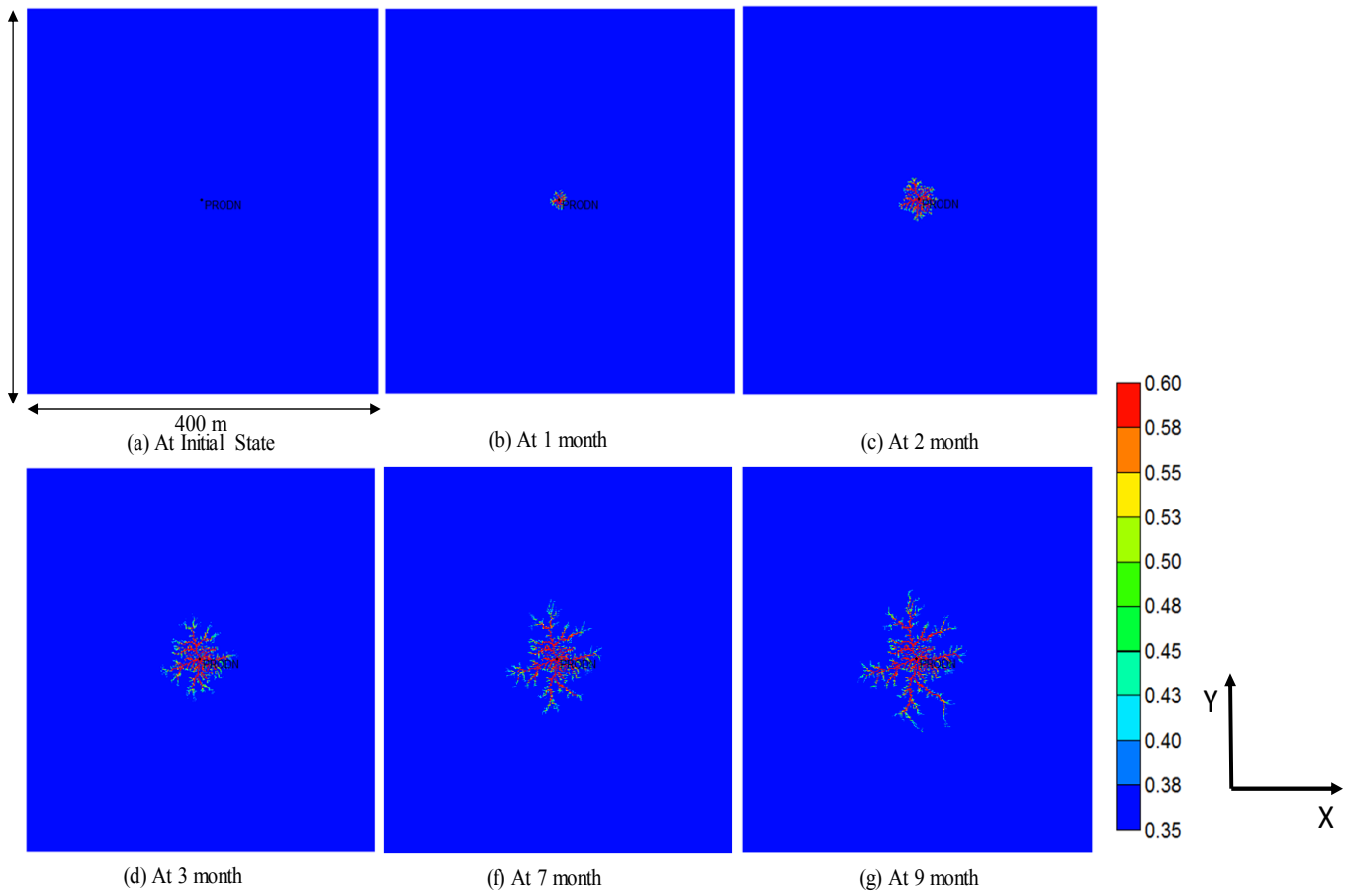

Figure 4-4: Top view of the porosity distribution in the middle (wormhole) layer at different times (Critical pressure gradient = 50.06 kPa/m)

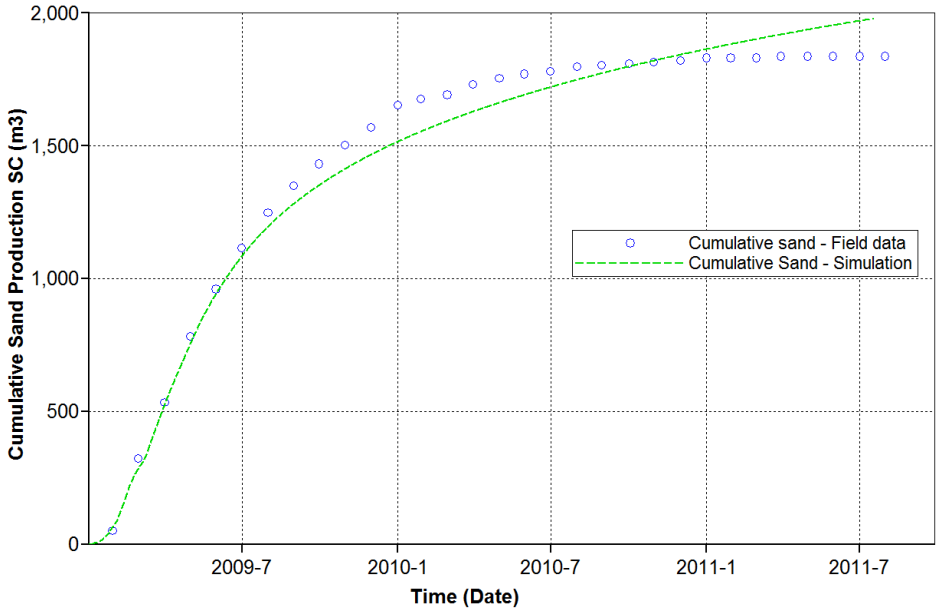

Figure 4-5: Comparison of cumulative sand production with the field historical data

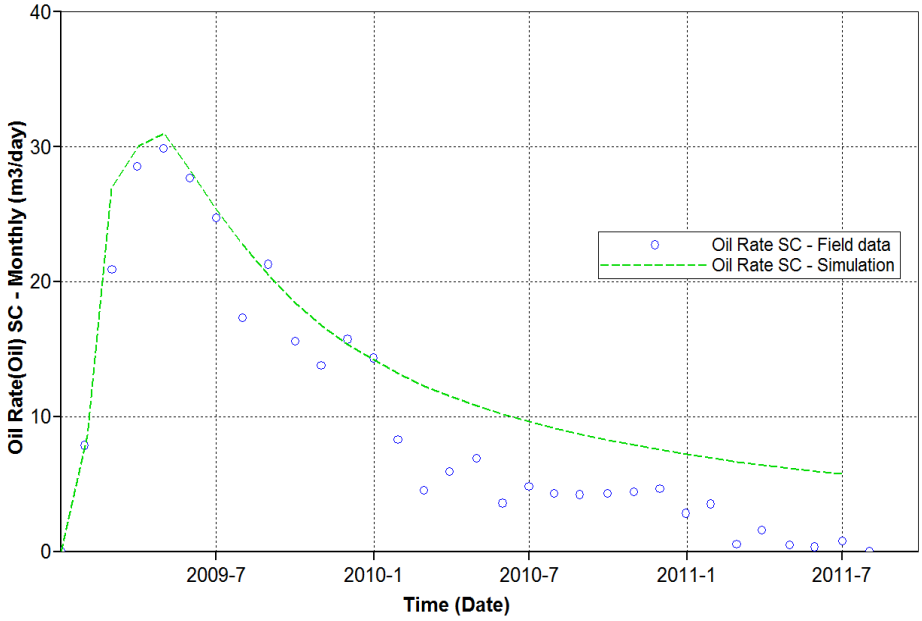

Figure 4-6: Comparison of monthly oil production with the field historical data

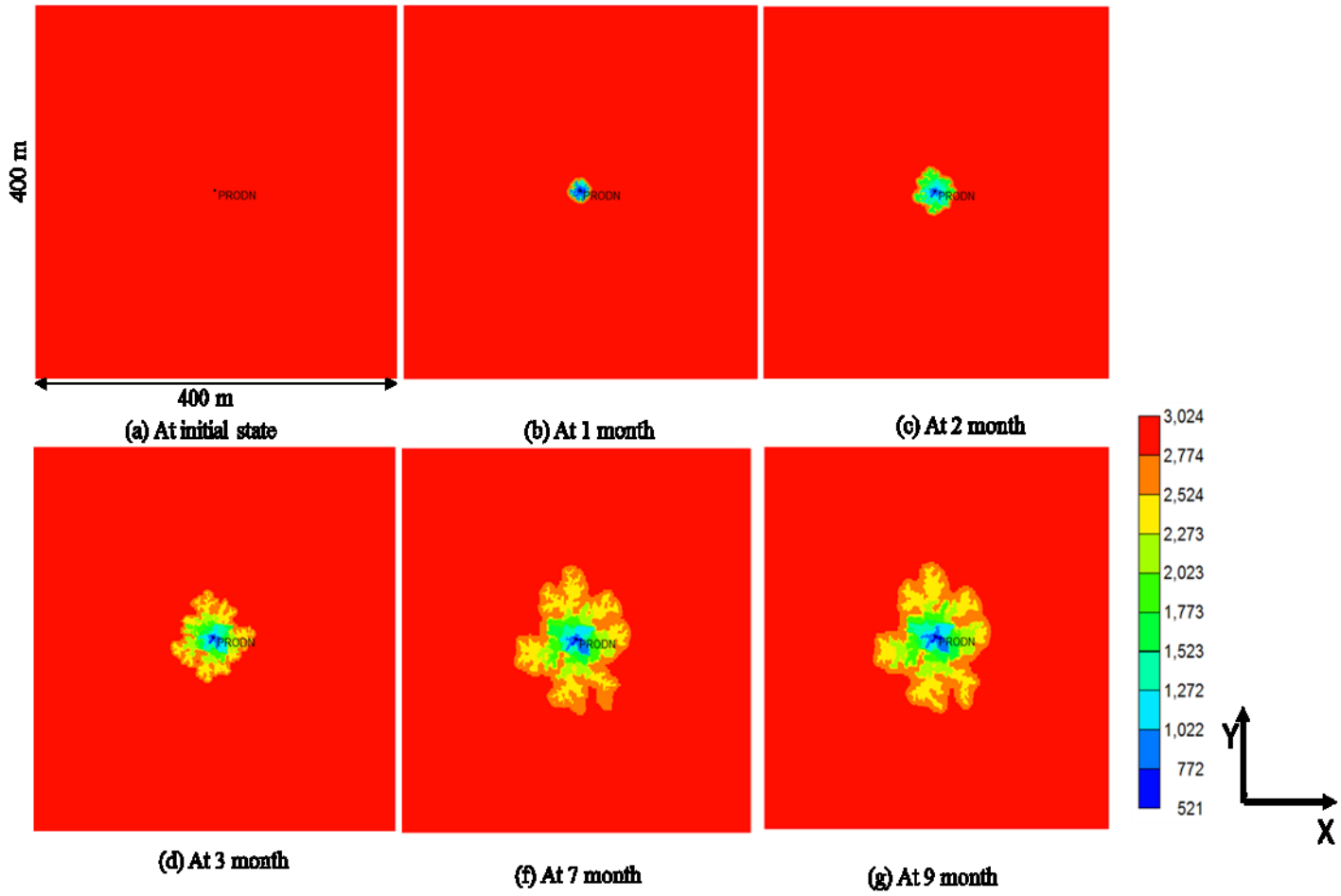

Figure 4-7: Top view of the pressure distribution in the middle (wormhole) layer at different times (Initial reservoir pressure = 3000 kPa & Bottomhole pressure = 500 kPa)

4.3.2 Model Validation through History Matching

As mentioned previously, a randomly selected fractal pattern is integrated with the geo-mechanical constraints to simulate the dynamic wormhole growth model. Therefore, several parameters, including *f* in the critical pressure gradient computation, wormhole permeability, foamy oil kinetic reaction parameters, are adjusted to match the field production data.

To avoid time-consuming coupling process or miss to capture the key point of wormhole growth, cumulative sand history data has been analyzed to figure out the coupling time step defined in the

coupling strategy. Records have indicated that about 781.89 m^3 of sand in the first four months, which accounts for 42.60% of cumulative sand production. Accordingly, we prefer to define a smaller coupling time step during the first four months, and then increase the coupling time steps to avoid computational time-consuming. On the other hand, the dye test results proposed by Squires (1993) indicated that the range of the wormhole network is about 200 m. Then we can simplify the shape of the 2D wormhole network as a circle on top view. According to the dimension of each grid, an estimated coupling time step can be calculated by the 40% circle area differential. The coupling time steps defined as 0.9 days at the first four months and then 1.8 days on our base field case. This parameter will be tuned slightly at a different time based on the field history data.

The history matching results of the monthly oil and cumulative sand production are shown in **Figure 4-8** & **4-9**, respectively. The values presented previously in **Table 4-1** are those obtained after the history matching process. The same wormhole permeability and foamy oil kinetics are used, and the figure intends to illustrate the sensitivity to different values of the critical pressure gradient on the final match. The practical range for the critical pressure gradient corresponding to the sand-arch-stability criterion is estimated to be 45-60 kPa/m. It should be noted that the critical pressure gradient is the key factor controlling the growth (i.e., lateral extent and rate) of a given wormhole network.

The simulation predictions offer a close match to actual field data. To verify the simulation result, the production profiles are compared to those obtained in other modeling studies, where the production data gathered from the same CHOPS well was also used. The cumulative sand production and oil rate predictions from Istchenko and Gates (2012) and Fan and Yang (2017) are also plotted in **Figure 4-10** & **4-11**. In Istchenko and Gates (2012), an extended wellbore model

(section 2.5) was employed, while in Fan and Yang (2017), the wellbore network is represented as a near wellbore region with enhanced permeability (section 2.5).

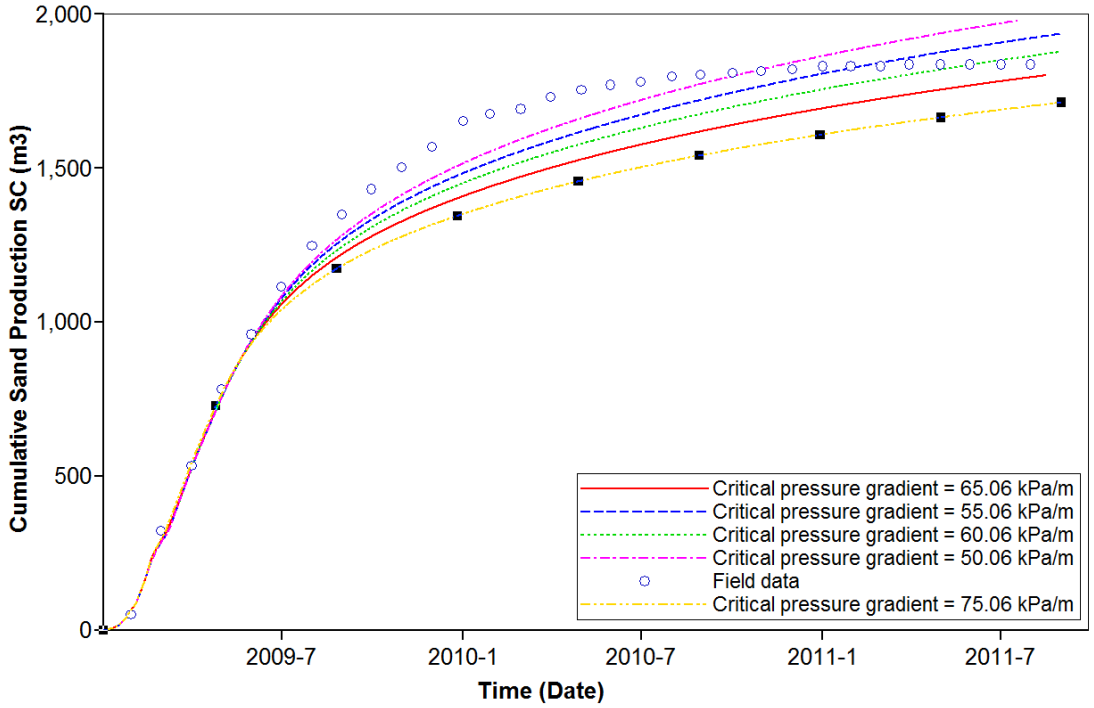

Figure 4-8: History matching of the cumulative sand production of a CHOPS well in the Cold Lake field. Five different critical pressure gradient levels are shown.

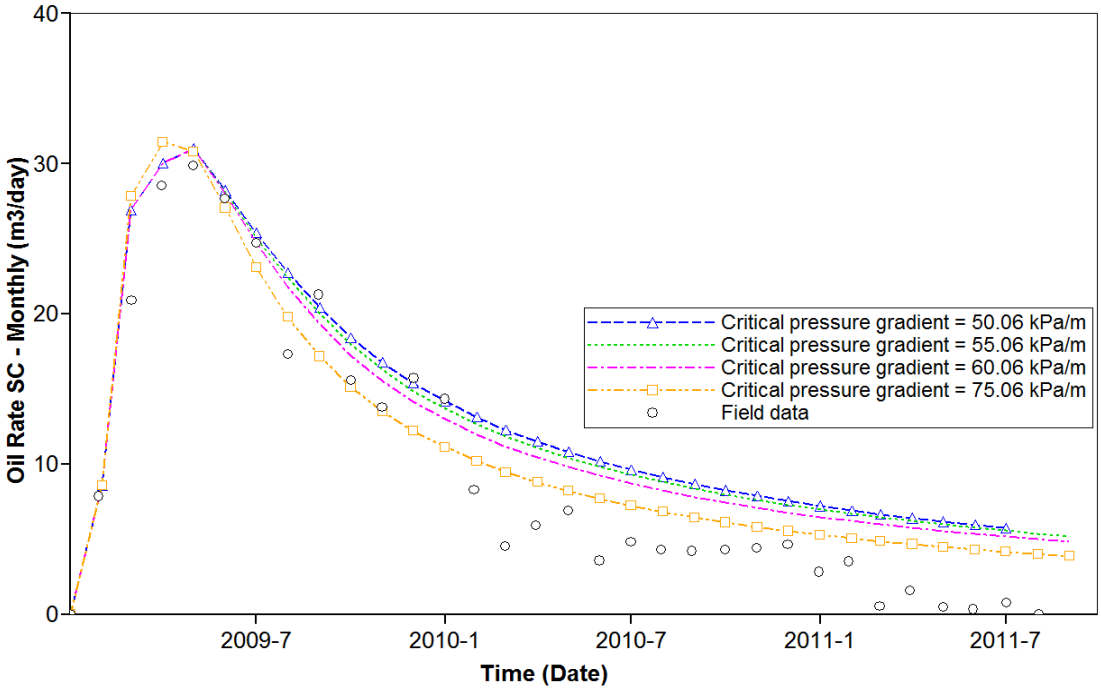

Figure 4-9: History matching of the Oil production rate of a CHOPS well in the Cold Lake field. Five different critical pressure gradient levels are shown.

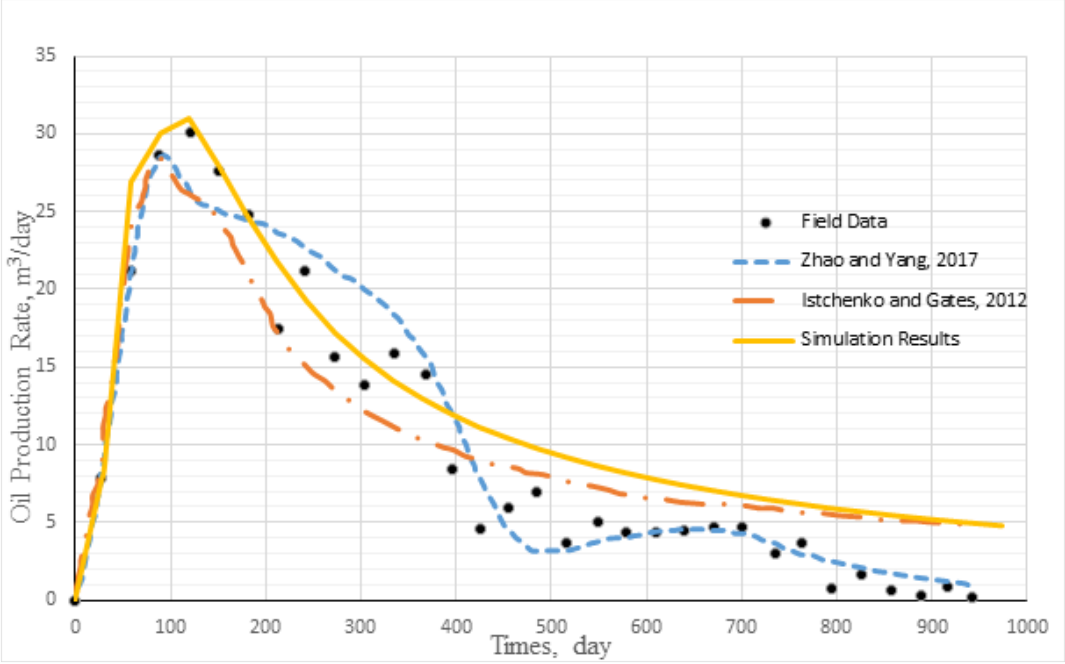

Figure 4-10: Comparison with other modeling approaches in terms of oil production rate for the same CHOPS well in the Cold Lake field

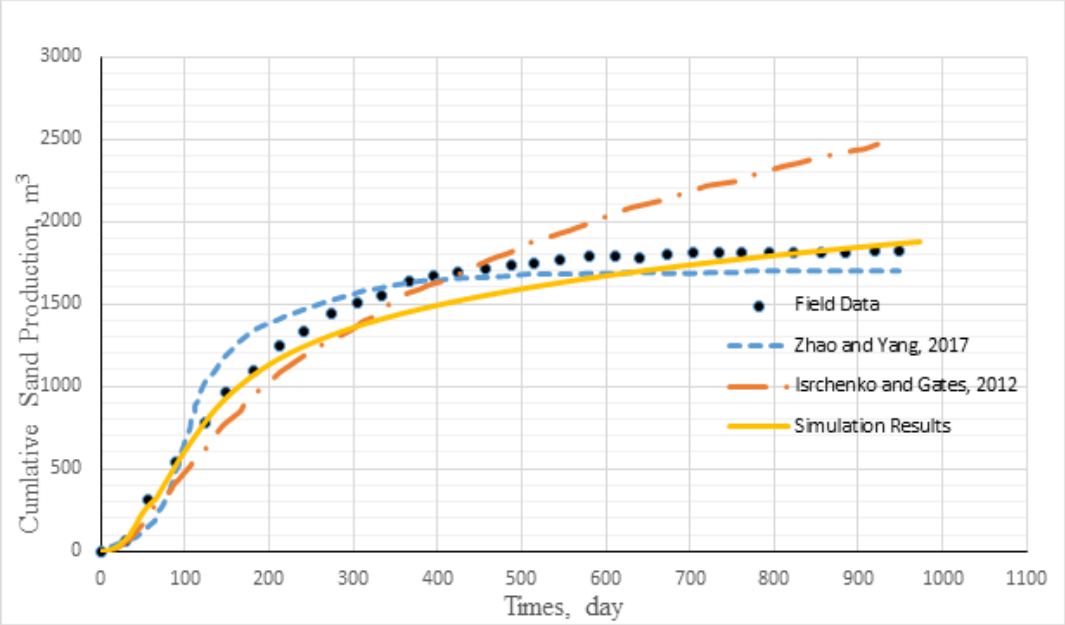

Figure 4-11: Comparison with other modeling approaches in terms of cumulative sand production for the same CHOPS well in the Cold Lake field

4.3.3 Sensitivity to Prescribed Fractal Patterns

In the analysis presented in the previous section, a single randomly selected fractal pattern was used to match the production histories for the field case. The simulation results and wormhole growth patterns obtained from the new workflow are reasonable. In this section, the simulations are repeated with several different fractal patterns, while keeping the rest of the model parameters to be the same as those presented in **Table 4-1**. Some examples of the prescribed fractal patterns are depicted in **Figure 4-12**. These models differ primarily in the directions of anisotropy or wormhole propagation.

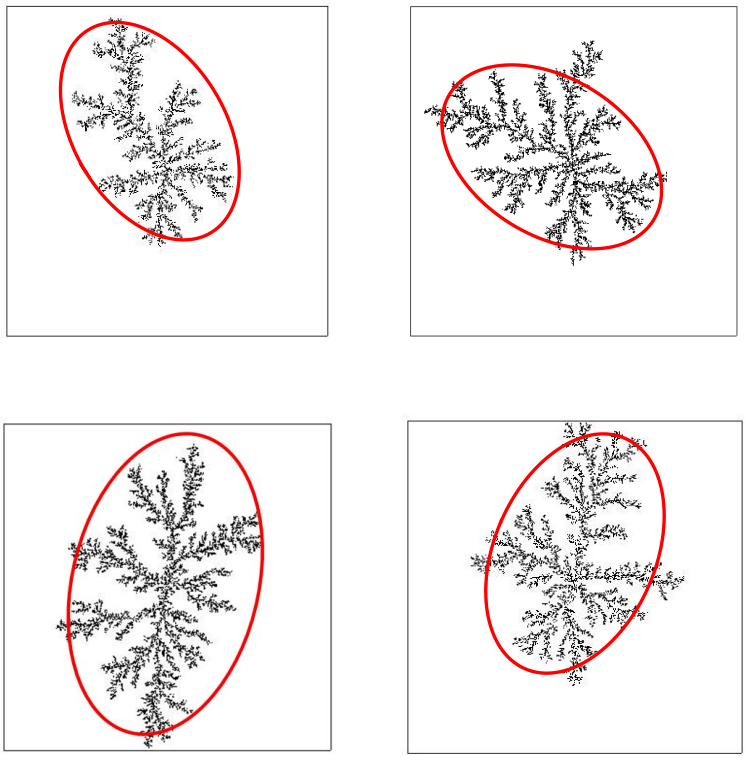

Figure 4-12: Multiple realizations of prescribed fractal patterns generated by the DLA model (The red circle presents the main direction of the prescribed wormhole networks.)

Figures 4-13 & 4-14 show the simulation results corresponding to two additional prescribed fractal pattern realizations, in comparison to the base case (critical pressure gradient = 50.06 kPa/m or f = 0.75) obtained from the previous section. Realization 2 gives similar results, in terms of cumulative sand production and oil monthly rate profiles, as in the original initial history-matched base case. Meanwhile, realization 1 shows less cumulative sand production as well as the oil production. For each realization of the realistic wormhole networks will result in the heterogeneous distribution of the petrophysical properties, which contributes the less production of sand and oil. However, the trends of cumulative sand production and oil rate of realization 1 show a good agreement with the field data. The final wormhole networks at the end of 12 months for each

realization are shown in **Figure 4-15**. The total drainage sizes resulted from these different realizations appear to be approximately the same as that corresponding to the base case, considering that the cumulative oil production volumes are similar for all 3 patterns. Given that history-matching is generally an ill-posed inverse problem, the actual wormhole pattern is likely to be uncertain; in other words, different realizations of the wormhole patterns may yield the same production profiles. However, the proposed workflow can be used to constrain multiple realizations of the fractal wormhole pattern to the CHOPS production histories. Additional data, such as 4D seismic, petrophysical logs and well tests, can also be readily integrated to condition the initial/prescribed fractal patterns.

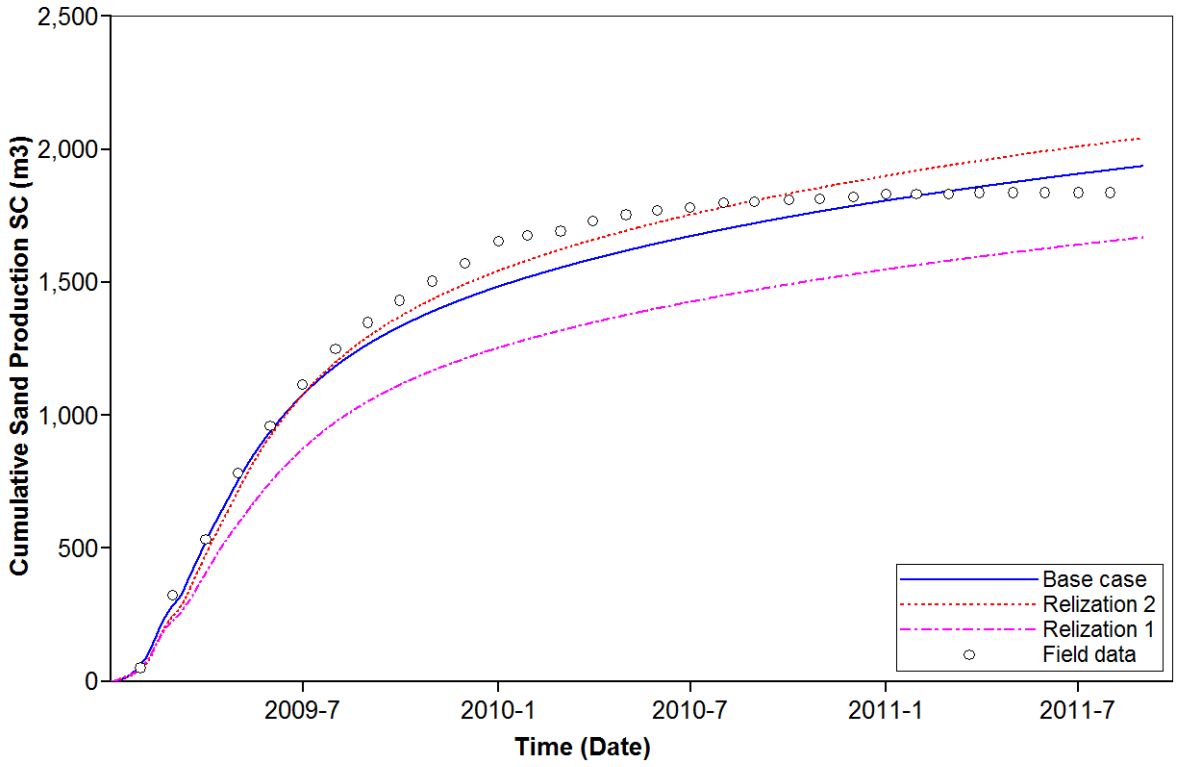

Figure 4-13: Comparison of cumulative sand production results for two more fractal pattern realizations

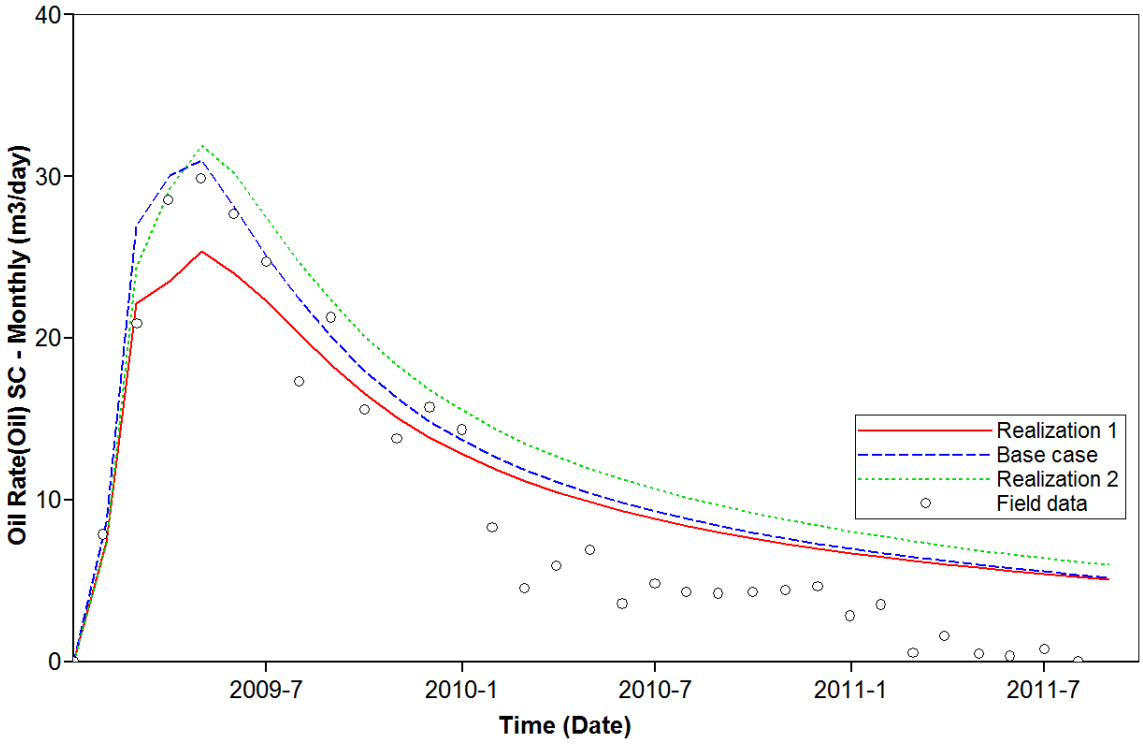

Figure 4-14: Comparison of oil production rate results for two more fractal pattern realizations

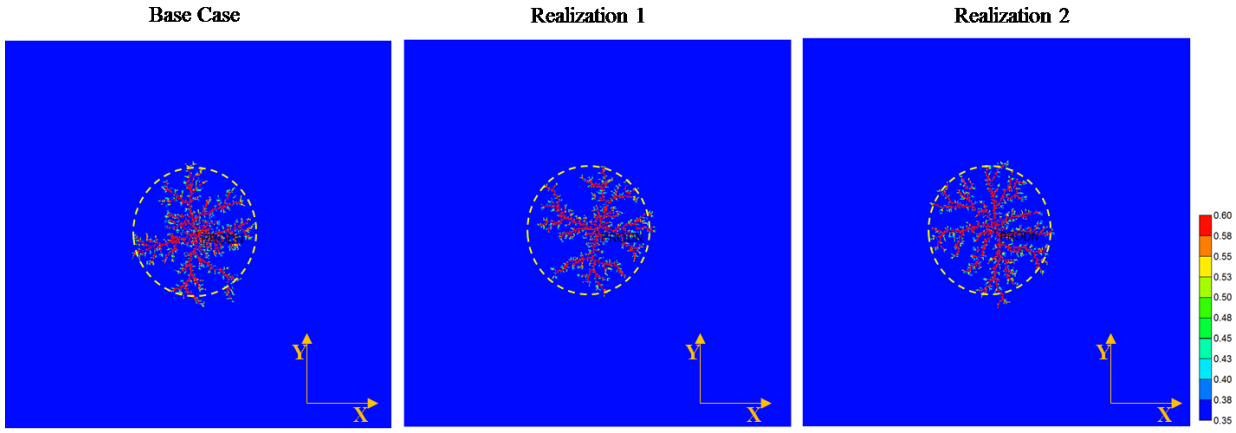

Figure 4-15: Top view of final porosity distribution for two other realizations

4.3.4 Impacts of Anisotropic Stress Distribution on Wormhole Networks

The main propagation direction of the wormholes is the results of multiple influencing factors. Recalling previous studies about the layer wormhole networks applied in our CHOPS model, the vertical principal stress becomes slightly larger than the horizontal stresses at a depth greater than 350 m. To examine the impacts of anisotropic stress distribution on the development of wormhole networks, another case (i.e., Case A), where anisotropic horizontal principal stresses, is examined. The principal horizontal stress gradient in the base case is 50.06 kPa/m. Therefore, for Case A, the maximum and minimum horizontal principle stresses gradient is set as 50.06 kPa/m and 20 kPa/m (~40% of the maximum value), respectively, as shown in **Figure 4-16** with the prescribed fractal pattern. The top views of the wormhole networks for the base case and Case A in the middle layer are compared in **Figure 4-17**. The cumulative sand production and monthly oil rate profiles for Case A are also presented in **Figure 4-17**. Due to the anisotropic stress distribution, the wormholes in case A tend to grow preferentially along the direction of minimum horizontal stress (as indicated in **Figure 4-17**).

In addition to in-situ stress distribution, there are several other contributing factors that could influence the direction of wormhole growth; for example, heterogeneous distribution of permeability, porosity, water saturation, and oil viscosity would have an influence on fluid flow, which is coupled with sand production. However, these factors are not considered in this thesis.

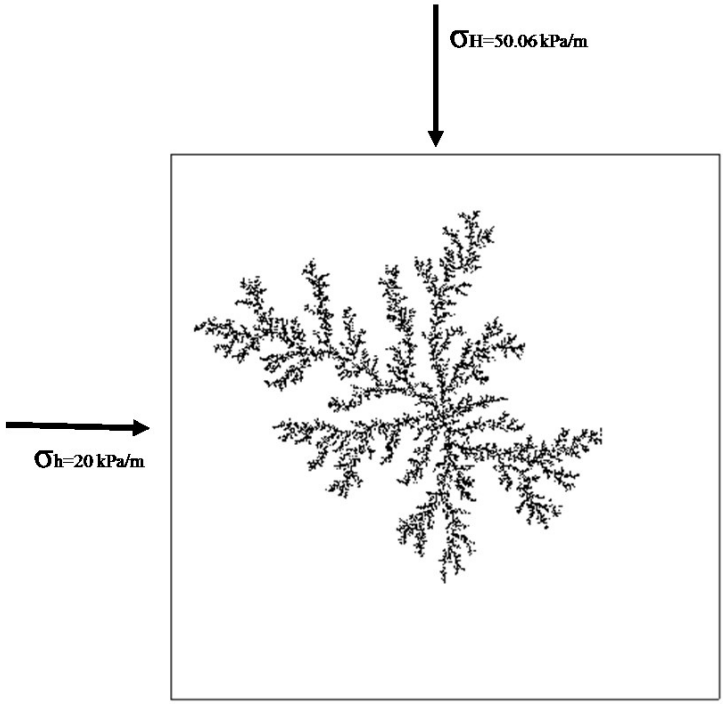

Figure 4-16: Two-dimensional view of horizontal stresses applied

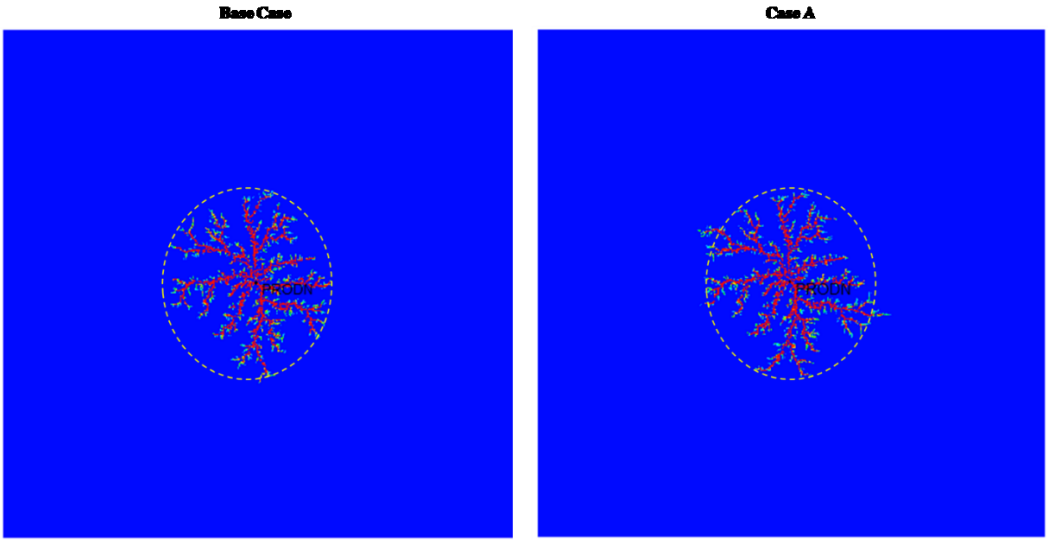

Figure 4-17: Effect of the anisotropic horizontal stress on wormhole networks (Porosity distribution map at final state; same elliptical area of each diagram)

4.4 Summary

In summary, the proposed simulation workflow is implemented to simulate the oil and sand production for a typical CHOPS well. The model is calibrated based on actual published field data, and the results are consistent with those obtained with other existing modeling approaches. However, the main advantage of this workflow is that the realistic wormhole growth paths are captured, with sand failure and fluidization being controlled by geo-mechanical constraints. In addition, the wormhole paths exhibit the appropriate fractal characteristics, which are commonly adopted for describing sand failure patterns. The workflow can be used to predict the spatial distribution of wormhole networks in practical field scale operations design. For example, in the case of multiple CHOPS wells, interference between numerous wormhole networks can be readily captured. It has been widely reported that wormholes developed from individual wells would often interfere and communicate.

Chapter 5. Conclusions and Recommendations for Future Work

5.1 Overview

A novel dynamic wormhole growth model is presented in this thesis to model the CHOPS process. It has the capacity to capture the main mechanisms of the CHOPS process, including foamy oil flow, sand failure, and fluidization, as well as the spatial distribution of wormhole networks. The model is implemented to model a field case study. The key conclusions and recommendation for future work are presented in this chapter.

5.2 Conclusions

1. The workflow proposed in this thesis provides a practical approach to model the CHOPS process, in which a realistic wormhole growth path being controlled by geomechanical constraints is integrated. It can be readily integrated with commercial reservoir simulators. The wormhole network is updated dynamically by coupling a sand failure criterion module with a fractal pattern to model the wormhole propagation into the reservoir. Important mechanisms including foamy oil flow and the sand fluidization are also integrated into the simulation procedure.
2. A main novelty of this work is that, in contrast to many existing wormhole modeling approaches, the developed workflow predicts a realistic wormhole growth path that follows

fractal statistics, while honoring the sand failure and fluidization physics, as controlled by geo-mechanical constraints.

3. The workflow is implemented to model an actual CHOPS well production in a field case study. The model is history matched using the field history data. The same data was also used in two other modeling studies in the literature, and the production profiles obtained from different approaches are compared. Despite a reasonable match in sand and oil production can be achieved with all three different modeling approaches, the proposed workflow is the only one that simulates a realistic fractal wormhole growth pattern. Other approaches that are based on the concepts of the extended wellbore or enhanced permeability in near wellbore region could only offer a simplified representation of the complex wormhole configurations. The detailed spatial distributions of wormholes predicted in this thesis are important inputs in practical field-scale operation design.
4. Many factors, such as heterogeneous distributions of the petrophysical and fluid properties (e.g., permeability, porosity, and oil viscosity) and anisotropic stress distribution, could impact the preferential wormhole growth direction. In this thesis, sensitivity of the growth pattern due to the anisotropic stress distribution is examined. The model predicts that the wormholes would tend to grow along the direction of minimum principal stress.
5. The proposed workflow can be used to constrain multiple realizations of the fractal wormhole pattern to the CHOPS production data, enabling the assessment of CHOPS performance due to uncertainty in the final developed wormhole networks.
6. Continuing sand production and wormhole network growth is essential to increasing the overall oil recovery factor during CHOPS. It, to some extent, is an indispensable factor to achieve a higher oil production.

7. When selecting infill well locations, inter-well communication through the wormhole network should be considered. The workflow presented in this thesis can be directly extended to model multiple CHOPS wells and examine potential interference between the wells.

5.3 Future Work

Based on the research documented in this thesis, the recommendation for future work listed below:

1. Around 90% of the heavy oil remains in the ground after the CHOPS process becomes uneconomic, marking it is necessary to have the enhanced oil recovery follow-up process. It is recommended that the novel CHOPS model proposed in this thesis can be used to simulate the follow-up EOR process, referred to post-CHOPS after field history matched.
2. In this research, results of a single well case model are in good agreement with the field history data. However, the workflow should be tested to simulate the interaction between multiple wells. It would be highly relevant in practical field-scale operations design.

Bibliography

Han, G.A.N.G., Bruno, M.I.K.E. and Dusseault, M.B., 2007. How much oil you can get from CHOPS. *Journal of Canadian Petroleum Technology*, *46*(04).

Geilikman, M.B., 1999. Sand production caused by foamy oil flow. *Transport in Porous Media*, *35*(2), pp.259-272.

Loughead, D.J. and Saltuklaroglu, M., 1992, March. Lloydminster heavy oil production: Why so unusual. In *9th Annual Heavy Oil and Oil Sands Technology Symposium, Calgary* (Vol. 11).

Tremblay, B., Sedgwick, G. and Vu, D., 1998, January. CT imaging of wormhole growth under solution-gas drive. In *SPE/DOE Improved Oil Recovery Symposium*. Society of Petroleum Engineers.

Smith, G.E., 1988. Fluid flow and sand production in heavy-oil reservoirs under solution-gas drive. *SPE Production Engineering*, *3*(02), pp.169-180.

Yeung, K.C. and Adamson, M.F., 1992. Burnt Lake Project-Bitumen production from the Cold Lake oil sands deposit without steam. *Fueling the Future: New Horizons in Oil Sands, Heavy Oil and Enhanced Oil Recovery, Calgary, Alberta, Canada*.

Metwally, M. and Solanski, S.C., 1995, January. Heavy Oil Reservoir Mechanisms, Lindbergh and Frog Lake Fields, Alberta Part I: Field Observations and Reservoir Simulation. In *Annual Technical Meeting*. Petroleum Society of Canada.

Istchenko, C.M. and Gates, I.D., 2014. Well/wormhole model of cold heavy-oil production with sand. *Spe Journal*, *19*(02), pp.260-269.

Rivero, J.A., Coskuner, G., Asghari, K., Law, D.H.S., Pearce, A., Newman, R., Birchwood, R.A., Zhao, J. and Ingham, J.P., 2010, January. Modeling CHOPS using a coupled flow-geomechanics simulator with nonequilibrium foamy-oil reactions: A multiwell history matching study. In *SPE Annual Technical Conference and Exhibition*. Society of Petroleum Engineers.

Liu, X. and Zhao, G., 2005. A fractal wormhole model for cold heavy oil production. *Journal of Canadian Petroleum Technology*, *44*(09).

Sawatzky, R.P., Lillico, D.A., London, M.J., Tremblay, B.R. and Coates, R.M., 2002, January. Tracking cold production footprints. In *Canadian International Petroleum Conference*. Petroleum Society of Canada.

Huang, W.S., Marcum, B.E., Chase, M.R. and Yu, C.L., 1997, January. Cold production of heavy oil from horizontal wells in the Frog Lake Field. In *International Thermal Operations and Heavy Oil Symposium*. Society of Petroleum Engineers.

Tremblay, B., Sedgwick, G. and Forshner, K., 1996, January. Modelling of sand production from wells on primary recovery. In *Annual Technical Meeting*. Petroleum Society of Canada.

Tremblay, B., Sedgwick, G. and Vu, D., 1998, January. CT imaging of wormhole growth under solution-gas drive. In *SPE/DOE Improved Oil Recovery Symposium*. Society of Petroleum Engineers.

Tremblay, B. and Oldakowski, K., 2002. Wormhole growth and interaction in a large sand pack. *Journal of Petroleum Science and Engineering*, *34*(1-4), pp.13-34.

Tremblay, B. and Oldakowski, K., 2003. Modeling of wormhole growth in cold production. *Transport in porous media*, *53*(2), pp.197-214.

Tremblay, B., 2005. Modelling of sand transport through wormholes. *Journal of Canadian Petroleum Technology*, *44*(04).

Tremblay, B., 2009. Cold flow: a multi-well cold production (CHOPS) model. *Journal of Canadian Petroleum Technology*, *48*(02), pp.22-28.

Squires, A., 1993, March. Inter-well tracer results and gel blocking program. In *The 10th Annual Heavy Oil and Oil Sands Technical Symposium, Calgary, Alberta, Canada, Mar*(Vol. 9).

Jensen, E., 1995, June. Primary Production Enhancement in Unconsolidated Sandstones. In *Paper SPE 30237 presented at the 1995 SPE International Heavy Oil Symposium, Calgary, Alberta, Canada* (pp. 19-21).

Yeung, K.C., 1995. *Cold flow production of crude bitumen at the Burnt Lake Project, northeastern Alberta* (No. CONF-9502114-Vol. 1). UNITAR, New York, NY (United States).

Metwally, M. and Solanski, S.C., 1995, January. Heavy Oil Reservoir Mechanisms, Lindbergh and Frog Lake Fields, Alberta Part I: Field Observations and Reservoir Simulation. In *Annual Technical Meeting*. Petroleum Society of Canada.

Lillico, D.A., Babchin, A.J., Jossy, W.E., Sawatzky, R.P. and Yuan, J.Y., 2001. Gas bubble nucleation kinetics in a live heavy oil. *Colloids and Surfaces A: Physicochemical and Engineering Aspects*, *192*(1-3), pp.25-38.

Uddin, M., 2005, January. Numerical studies of gas exsolution in a live heavy oil reservoir. In *SPE International Thermal Operations and Heavy Oil Symposium*. Society of Petroleum Engineers.

Maini, B.B., 2001. Foamy-oil flow. *Journal of Petroleum Technology*, *53*(10), pp.54-64.

Treinen, R.J., Ring, W.W., Spence, A.P., de Mirabal, M. and Huerta, M., 1997, January. Hamaca: Solution gas drive recovery in a heavy oil reservoir, experimental results. In *Latin American and Caribbean Petroleum Engineering Conference*. Society of Petroleum Engineers.

Sahni, A., Gadelle, F., Kumar, M., Kovscek, A.R. and Tomutsa, L., 2001, January. Experiments and Analysis of Heavy Oil Solution Gas Drive. In *SPE Annual Technical Conference and Exhibition*. Society of Petroleum Engineers.

Wieland, D.R. and Kennedy, H.T., 1957. Measurements of bubble frequency in cores. *Trans. AIME*, *210*, pp.122-125.

Ahmed, T. and Behavior, H.P., 1989. Gulf Publishing Company. *Houston, Texas*, *250*.

Batycky, J.P., Leaute, R.P. and Dawe, B.A., 1997, January. A mechanistic model of cyclic steam stimulation. In *International thermal operations and heavy oil symposium*. Society of Petroleum Engineers.

Treinen, R.J., Ring, W.W., Spence, A.P., de Mirabal, M. and Huerta, M., 1997, January. Hamaca: Solution gas drive recovery in a heavy oil reservoir, experimental results. In *Latin American and Caribbean Petroleum Engineering Conference*. Society of Petroleum Engineers.

Theofanous, T., Biasi, L., Isbin, H.S. and Fauske, H., 1969. A theoretical study on bubble growth in constant and time-dependent pressure fields. *Chemical Engineering Science*, *24*(5), pp.885-897.

Szekely, J. and Martins, G.P., 1971. Non-equilibrium effects in the growth of spherical gas bubbles due to solute diffusion. *Chemical Engineering Science*, *26*(1), pp.147-159.

Kraus, W.P., McCaffrey, W.J. and Boyd, G.W., 1993, January. Pseudo-bubble point model for foamy oils. In *Annual Technical Meeting*. Petroleum Society of Canada.

Lebel, J.P., 1994, March. Performance implications of various reservoir access geometries. In *11th Annual Heavy Oil & Oil Sands Tech. Symp., March* (Vol. 2).

Kumar, R. and Pooladi-Darvish, M., 2002. Solution-gas drive in heavy oil: field prediction and sensitivity studies using low gas relative permeability. *Journal of Canadian Petroleum Technology*, *41*(03).

Pooladi-Darvish, M. and Firoozabadi, A., 1999. Solution-gas drive in heavy oil reservoirs. *Journal of Canadian Petroleum Technology*, *38*(04).

Claridge, E.L., 1994. A proposed model and mechanism for anomalous foamy heavy oil behavior.

Elkins, L.F., Morton, D. and Blackwell, W.A., 1972, January. Experimental fireflood in a very viscous oil-unconsolidated sand reservoir, SE Pauls Valley Field, Oklahoma. In *Fall Meeting of the Society of Petroleum Engineers of AIME*. Society of Petroleum Engineers.

Geilikman, M.B. and Dusseault, M.B., 1997. Fluid rate enhancement from massive sand production in heavy-oil reservoirs. *Journal of Petroleum Science and Engineering*, *17*(1-2), pp.5-18.

Bratli, R.K. and Risnes, R., 1981. Stability and failure of sand arches. *Society of Petroleum Engineers Journal*, *21*(02), pp.236-248.

Wang, J., Walters, D., Wan, R.G. and Settari, A., 2005, January. Prediction of volumetric sand production and wellbore stability analysis of a well at different completion schemes. In *Alaska Rocks 2005, The 40th US Symposium on Rock Mechanics (USRMS)*. American Rock Mechanics Association.

Shao, J.F. and Marchina, P., 2002, January. A damage mechanics approach for the modelling of sand production in heavy oil reservoirs. In *SPE/ISRM Rock Mechanics Conference*. Society of Petroleum Engineers.

Yuan, J.Y., Tremblay, B. and Babchin, A., 1999. A wormhole network model of cold production in heavy oil. In *SPE international thermal operations and heavy oil symposium* (pp. 153-159).

Rangriz Shokri, A. and Babadagli, T., 2012, January. An approach to model CHOPS (Cold Heavy Oil Production with Sand) and post-CHOPS applications. In *SPE Annual Technical Conference and Exhibition*. Society of Petroleum Engineers.

Denbina, E.S., Baker, R.O., Gegunde, G.G., Klesken, A.J. and Sodero, S.F., 2001. Modelling cold production for heavy oil reservoirs. *Journal of Canadian Petroleum Technology*, *40*(03).

Chang, J. and Ivory, J., 2013. Field-scale simulation of cyclic solvent injection (CSI). *Journal of Canadian Petroleum Technology*, *52*(04), pp.251-265.

Haddad, A.S. and Gates, I., 2015. Modelling of Cold Heavy Oil Production with Sand (CHOPS) using a fluidized sand algorithm. *Fuel*, *158*, pp.937-947.

Witten Jr, T.A. and Sander, L.M., 1981. Diffusion-limited aggregation, a kinetic critical phenomenon. *Physical review letters*, *47*(19), p.1400.

Feder, J., 1988. The Cluster Fractal Dimension. In *Fractals*(pp. 31-40). Springer, Boston, MA.

Meakin, P., 1987. Diffusion-limited aggregation on multifractal lattices: A model for fluid-fluid displacement in porous media. *Physical Review A*, *36*(6), p.2833.

Selinger, R.B., Nittmann, J. and Stanley, H.E., 1989. Inhomogeneous diffusion-limited aggregation. *Physical Review A*, *40*(5), p.2590.

Chang, J., Ivory, J. and London, M., 2015, June. History Matches and Interpretation of CHOPS Performance for CSI Field Pilot. In *SPE Canada Heavy Oil Technical Conference*. Society of Petroleum Engineers.

Fan, Z. and Yang, D., 2017, February. Quantification of Sand Production by Use of a Pressure-Gradient-Based Sand Failure Criterion. In *SPE Canada Heavy Oil Technical Conference*. Society of Petroleum Engineers.